TECHNISCHE UNIVERSITÄT WIEN
Vienna University of Technology

# Detection of Neuronal Activities Using Genetically Encoded Calcium and Voltage Indicators

DIPLOMARBEIT

zur Erlangung des akademischen Grades

**Diplom-Ingenieur**

im Rahmen des Studiums

**Biomedical Engineering**

eingereicht von

**Dipl.-Ing. Markus Michael Hilscher, BSc.**
Matrikelnummer 0727932

an der
Fakultät für Mathematik und Geoinformation der Technischen Universität Wien

Betreuer: DDDr. Frank Rattay
Institut für Analysis und Scientific Computing, Technische Universität Wien
Co-Betreuer: Dr. Richardson Naves Leão
Neurodynamics Lab, Department of Neuroscience, Uppsala University

Wien, 03.05.2013

(Unterschrift Verfasser) (Unterschrift Betreuer)

# Erklärung zur Verfassung der Arbeit

Dipl.-Ing. Markus Michael Hilscher, BSc.
[redacted]

Hiermit erkläre ich, dass ich diese Arbeit selbständig verfasst habe, dass ich die verwendeten Quellen und Hilfsmittel vollständig angegeben habe und dass ich die Stellen der Arbeit - einschließlich Tabellen, Karten und Abbildungen -, die anderen Werken oder dem Internet im Wortlaut oder dem Sinn nach entnommen sind, auf jeden Fall unter Angabe der Quelle als Entlehnung kenntlich gemacht habe.

(Ort, Datum) (Unterschrift Verfasser)

# Acknowledgements

I would like to express the deepest appreciation to everyone who followed and supported me during my academic formation and especially during this diploma thesis.

First and foremost, it gives me great pleasure in acknowledging the support and help of my supervisor Professor DDDr. Frank Rattay from the Vienna University of Technology, who has guided me through my scientific career since the very beginning of my studies. I got to know Professor Rattay as a very dedicated person, who offered his continuous advice, encouragement and motivation during my diploma thesis. I could always discuss all my scientific and personal issues with him and he undoubtedly advocated my plan of going abroad for experimental research at the University of Uppsala.

It is with immense gratitude that I acknowledge the support of Professor Dr. Richardson Naves Leão, who supervised my scientific projects and this thesis at the University of Uppsala. He introduced me to lab work and taught me electrophysiology with a lot of patience and enthusiasm. During the past two years and under his supervision I acquired experience with various techniques, including patch clamp and fluorescence microscopy. After I expressed my intention to work on the interface between theory and experimental research, he made it possible for me to study at the Federal University of Rio Grande do Norte in Brazil.

In this regard I want to thank the International Office of the Vienna University of Technology for supporting me with a grant which made it easy for me to study abroad.

Furthermore, I want to thank my international friends who always made me feel welcome in their countries. Building bridges, both at home and abroad means a lot to me. I will never forget all the fascinating adventures we had together.

One of these special friends I want to explicitly mention here, is Hermany Munguba, who I got to know during my very first days in Uppsala. Especially his support with the cell cultures and figures was essential for this thesis and his motivating presence when recording the experiments was of great importance.

Finally, I owe my deepest gratitude to my parents Silvia and Wilfried as well as my brother Bernhard who always supported me during my studies. They have always provided me with the best conditions in order to achieve maximal success.

# Abstract

**Objectives:** Understanding the dynamics of neuronal networks will require the ability of monitoring action potentials and synaptic activities in identified neuronal populations. However, the increasing number of optogenetic reporters and the lack of comparisons under identical conditions have generated the difficulty of choosing the most appropriate indicator for assessing the activity of individual neurons or whole networks.

**Methods:** While genetically encoded calcium indicators provide larger dynamic ranges and a higher signal-to-noise ratio, genetically encoded voltage indicators offer faster kinetics and are able to detect single action potentials through their fluorescence change. Thus, both classes of genetically encoded indicators provide different advantages and disadvantages. Up to date, no study has compared these two reporters. In this study we opposed the two calcium indicators GCaMP3 (as the most widely established) and R-GECO1 (for its far-red shifted fluorescence) to the voltage indicator VSFP-butterfly1.2 (for its fast kinetics) under similar experimental conditions.

**Results:** The genetically encoded reporters GCaMP3, R-GECO1 and VSFP-butterfly1.2 were successfully expressed in primary hippocampal neuron cultures in order to assess their fluorescence emission in response to membrane potential variations resulting from action potentials or synaptic inputs. Our experiments demonstrated that the two calcium indicators have a higher signal-to-noise ratio in response to evoked action potentials, compared to the voltage indicator. However, the detection of action potentials was possible with all three reporters. Moreover, even ongoing neuronal network synchronization could be observed.

**Conclusion:** Our results shed light on how well genetically encoded indicators can report single action potentials and synaptic inputs by their fluorescence emission. Additionally, we show evidence that calcium indicators are not only able to monitor temporal differences of membrane changes but also provide a reliable spatial discrimination. We further demonstrate that the identification of active and silent neurons is easily possible using calcium reporters and that even synchronizing activities among neurons can be imaged.

# Kurzfassung

**Motivation:** Um die Dynamiken neuronaler Netzwerke verstehen zu können, wird die Überwachung von Aktionspotenzialen und synaptischen Aktivitäten in bestimmten neuronalen Populationen immer bedeutender. Allerdings machen die zunehmende Anzahl von optogenetischen Reportern und die fehlenden Vergleiche unter identischen Bedingungen die Auswahl des am besten geeigneten Indikators für die Beurteilung der Aktivität einzelner Neuronen oder vollständiger Netzwerke, immer schwieriger.

**Methoden:** Während genetisch kodierte Calcium-Indikatoren einen größeren dynamischen Bereich und ein höheres Signal-Rausch-Verhältnis haben, bieten genetisch kodierte Spannungs-Indikatoren eine schnellere Kinetik und sind in der Lage, einzelne Aktionspotentiale durch ihre Fluoreszenzveränderung zu erfassen. Somit bieten beide Klassen von genetisch kodierten Indikatoren unterschiedliche Vor- und Nachteile. Bis dato hat jedoch keine Studie diese beiden Reporter gegenübergestellt. In dieser Studie haben wir die beiden Calcium-Indikatoren GCaMP3 (als der am weitesten etablierte) und R-GECO1 (für seine tief-rote Fluoreszenz) mit dem Spannungs-Indikator VSFP-butterfly1.2 (für seine schnelle Kinetik) unter ähnlichen experimentellen Bedingungen vergleichen.

**Ergebnisse:** Die genetisch kodierten Reporter GCaMP3, R-GECO1 und VSFP-butterfly1.2 wurden erfolgreich in Nervenzellen des Hippocampus ausgeprägt, um ihre Fluoreszenzemission in Reaktion auf Membranpotential-Veränderungen, ausgelöst durch Aktionspotentiale oder synaptischen Signale, zu bewerten. Unsere Versuche zeigen, dass die beiden Calcium-Indikatoren ein höheres Signal-Rausch-Verhältnis in Reaktion auf evozierte Aktionspotentiale haben, im Vergleich zum Spannung-Indikator. Dennoch war der Nachweis von Aktionspotentialen mit allen drei Reportern möglich. Darüber hinaus konnte sogar stattfindende neuronale Netzwerk-Synchronisation beobachtet werden.

**Fazit:** Unsere Ergebnisse erläutern, wie gut genetisch kodierte Indikatoren einzelne Aktionspotenziale und synaptische Signale durch ihre Fluoreszenzemission berichten können. Zusätzlich haben wir Hinweise, dass Calcium-Indikatoren nicht nur in der Lage sind, zeitliche Unterschiede von Membranveränderungen zu überwachen, sondern auch eine zuverlässige räumliche Diskriminierung besitzen. Wir zeigen außerdem, dass die Identifizierung von aktiven und inaktiven Neuronen mit Calcium-Reportern möglich ist und dass selbst synchronisierende Aktivitäten zwischen Nervenzellen aufgezeichnet werden können.

# Contents

CHAPTER 1

# Introduction

## 1.1 Motivation

The brain is one of the most important organs in human bodies and controls functions ranging from simple such as breathing to more complex such as memory, learning and mental state. Our brains consist of billions of neurons which are connected in complex circuits and communicate with one another by electrical signals. One of the most challenging approaches in neuroscience today is to study the dynamics of the intact brain and the patterns of electrical activity. In order to understand the language of the brain, it is necessary to monitor signaling pathways with high spatio-temporal patterns. This means high resolution in the time dimension as well as high resolution in the space dimension is desired. Usually advanced electrophysiological methods such as the patch clamp technique or the sharp electrode technique are used to record from single neurons and / or multiple cells in order to investigate their activities. These are invasive recording techniques and require the insertion of microelectrodes into the tissue in order to be able to monitor electrical signals. An alternative approach is to use optical imaging based on organic fluorescent dyes, which allows to monitor neuronal activities in a relative non-invasive manner. However, organic fluorescent dyes are not the optimal technique for recording the activities of specific neurons. They are not suitable for chronic staining and can also be toxic for the cells.

To overcome these problems, genetically encoded indicators (GEIs) have been developed and emerge as a new area called *optogenetics* which combines the advantages of optics and genetics in order to control the activities of neurons. GEIs are fluorescent proteins which can be targeted to and expressed in specific cell populations. They do not need to be loaded onto cells as it is the case for fluorescent dyes but instead, their genes which encode these proteins can be transfected to defined cell lines which makes a proper targeting possible. Moreover, it is also feasible to breed transgenic mice which then express the fluorescent protein in specific cell populations. This is a non-negligible advantage of GEIs, since even subcellular compartments can be addressed. In addition to that, GEIs have recently reached both a high spatial and a high temporal resolution, making them very attractive for the monitoring of electrical signals in neurons.

Nowadays there is a huge amount of different optogenetic reporters available. We can distinguish two major classes: genetically encoded calcium indicators (GECIs) and genetically encoded voltage indicators (GEVIs). This increasing number of optogenetic reporters and the lack of comparisons of these indicators gave us the motivation to evaluate their potency of reporting neuronal activities. Up to date, no study has compared various GECIs and GEVIs under identical conditions. Thus, with this revolutionary study we want to give strong advice in order to overcome the rising difficulty of choosing the most appropriate reporter when answering questions in neuroscience.

## 1.2 Intention of the Approach

Both GECIs and GEVIs are engineered biosensors derived from the fusion of a fluorescent protein (FP) to a detector protein, which then is able to convert physiological signals into changes in fluorescence output. In this study we aim to evaluate two calcium indicators and one voltage-sensitive fluorescent protein (VSFP) in order to investigate which GEI suits better for answering different questions in neuroscience. It is assumed that GECIs provide a larger dynamic range and a higher signal-to-noise ratio (SNR) compared to GEVIs. On the other hand, GECIs are believed to provide only information about the occurrence of neuronal events, but do not allow the discrimination of single signals, called action potentials (APs), because of their slow kinetics. With GEVIs it seems to be possible to detect single APs, even in fast spiking neurons. Moreover, they allow the detection of subthreshold activities as well as synaptic inputs by their fluorescence emission.

Our study evaluates these properties for the calcium indicators GCaMP3 and R-GECO1 and the voltage-sensitive fluorescent protein VSFP-butterfly1.2. We show their performances in the detection of action potentials and synaptic inputs in cultured neurons. Therefore the three indicators were expressed in HEK293 cells and cultured hippocampal neurons in order to measure the effect of membrane potential changes by their fluorescence emission rates. This means that we measured the electrical properties of the fluorescent neurons by applying electrophysiological methods and simultaneously captured the fluorescence output with a very fast photodetector, as shown in Fig. 1.1.

Our experiments involved the implementation and transfection of neuronal cultures expressing the genetically encoded indicators, as well as the investigation of underlying electrophysiological properties. These properties might have changed when genetically modifying neurons. Therefore we tested these possible changes by performing real-time experiments and introducing specific ionic currents to the cells. Furthermore, we studied the fluorescence emission in response to APs, comparing evoked APs to spontaneous APs, varying the frequencies of the evoked APs and investigated the fluorescence output after synaptic activities. We also investigated how these three GEIs can be used in order to study synchronization of neuronal assemblies.

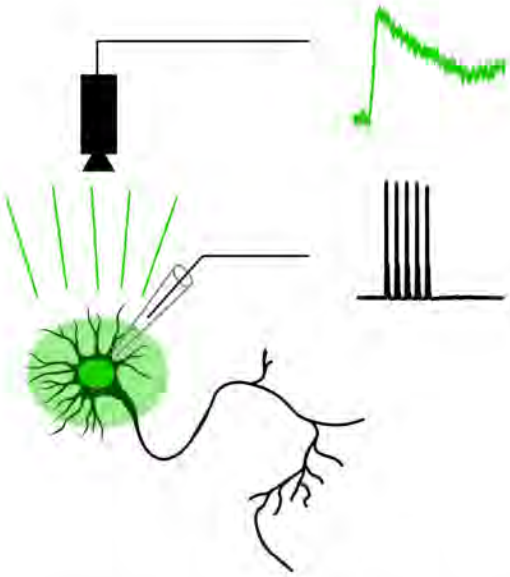

**Figure 1.1:** Experimental setup. Three different genetically encoded indicators were compared in order to evaluate which one reports neuronal membrane activities, such as action potentials or synaptic inputs, best by the fluorescence emission.

## 1.3 Organizational and Ethical Issues

This diploma thesis presents scientific results, achieved at the Institute for Analysis and Scientific Computing, Vienna University of Technology, Vienna, Austria and the Neurodynamics Lab, Department of Neuroscience, Uppsala University, Uppsala, Sweden. It includes both computational neuroscience aspects as well as electrophysiological recordings of hippocampal cultures. All animal experiments have been performed in accordance with the European Council Directive (86/609/EEC) and have been approved by Swedish Animal Welfare authorities. The experiments always follow Uppsala University guidelines for the care and usage of laboratory animals.

## 1.4 Structure of this Thesis

The chapters of this diploma thesis are organized as follows. Chapter 2 gives an introduction to the most prominent neuronal signals and how we can measure them. Chapter 3 describes the techniques needed in order to monitor these signals optically. Chapter 4 contains an overview of fluorescent proteins and how their excitation and emission spectra look like. Chapter 5 describes how to make cell cultures and investigates possible changes of cell properties due to the transfection with genetical material whereas chapter 6 contains the description and implementation of primary hippocampal neuron cultures. The remaining chapters 7, 8 and 9 present methods, results and a discussion.

CHAPTER 2

# Neuronal Signaling

This chapter introduces the fundamental signaling properties of neurons, including basic extracellular and intracellular mechanisms causing this typical shape of an action potential. Furthermore, it contains an overview of available electrophysiological methods for the measurement of these electrical phenomenas occurring in our nerve cells and it compares their advantages and disadvantages depending on the raised scientific question.

## 2.1 Nerve Cell Activities

The humans' most important and most complex organ is the brain. It contains billions of neurons which communicate with one another during day and night. A human brain oscillates during exploration, motion and learning. It is also active during sleep and when it is forming memories. Considering the electrical activities, our brains are usually very active, meaning that the neurons talk to one another almost all the time. A typical neuron consists of a cell body (also called *soma*), *dendrites*, which are usually branched projections transferring information to the cell body and an *axon*, which sends electrical impulses away from the neuron's soma (see Fig. 2.1 A). The connections between neurons are called *synapses*. This is the connecting terminal where information is sent from the *presynaptic* neuron to the *postsynaptic* one, from the sender to the receiver. The membrane of a neuron which separates the hydrophilic intracellular space from the hydrophilic extracellular space by a lipophilic bilayer has pores (ionic pumps and ion channels) included which are able to transport ions between the inside and the outside of a cell (see Fig. 2.1 B).

This mechanism maintains a voltage gradient across the membrane (the inside of a cell is usually more negative than the outside) and generates concentration differences of ions by active (ionic pumps) and passive (ionic channels) processes. The ions contributing to the transmembrane voltage (called membrane potential in the following) of a neuron are mainly sodium, potassium, chloride and calcium ions with higher extracellular concentrations for $Na^+$, $Cl^-$ and $Ca^{2+}$ and

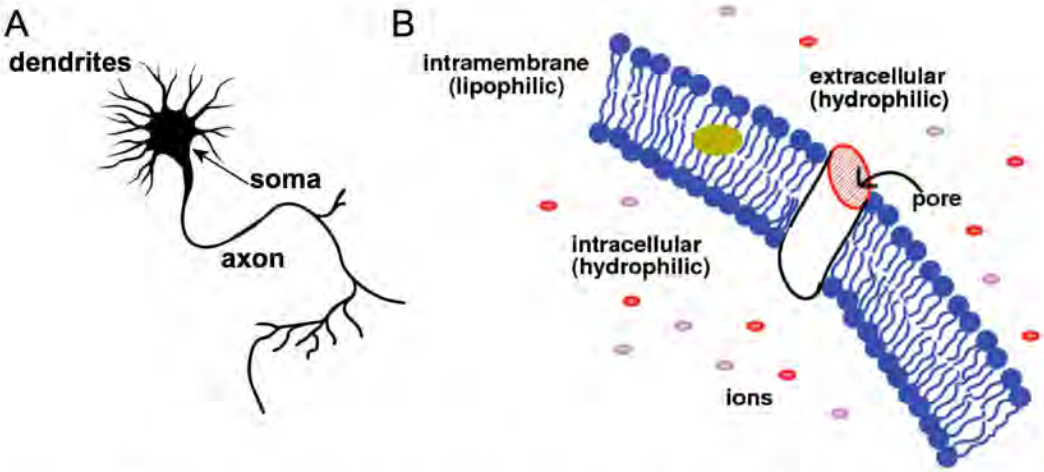


**Figure 2.1:** The neuron and its membrane. A: The schematic drawing shows the most important parts of a neuron, consisting of a soma, an axon and dendrites. B: The cell membrane (blue) has a lipid bilayer with membrane-spanning proteins (white), which can form pores or tunnels (red) that allow ions to move in or out of the cell. The intracellular and extracellular space are hydrophilic, the intramembrane space is lipophilic. The illustration is taken from [ Lytton and Kerr, (2006) ].

higher intracellular concentration for $K^+$. These four ions are not only involved in establishing the membrane potential when the neuron is in rest, but also play an essential role when neurons send information along their axons. This information is called *action potential* or *spike*. It is initiated at the axon initial segment, a part of the axon in the vicinity of the soma and travels along the axon to the synaptic terminal where it activates postsynaptic cells.

Action potentials are very short events in which the cell's membrane potential rapidly rises and falls, following a neuron specific trajectory (see Fig. 2.2). This typical shape of an action potential results from the following basic membrane mechanisms starting when the neuron is "quiet" and having a membrane potential between -60 $mV$ and -90 $mV$, also called *resting potential*. [ Purves et al., (2004) ]

1. **Weak depolarization:** An external signal, mostly an applied stimulus or a synaptic input leads to rise the intracellular $Ca^{2+}$ and/or $Na^+$ concentration.

2. **Fast depolarization:** At a neuron specific *threshold potential* (usually around -40 $mV$ to -20 $mV$) the voltage gated $Na^+$ channels open and the cell polarizes towards the reversal potential of $Na^+$ (usually around 60 $mV$) meaning that there is no flow of $Na^+$ ions from one side of the membrane to the other. Positive membrane potentials are called *overshoot*.

3. **Repolarization:** Voltage gated $K^+$ channels open and the membrane potential drops towards the reversal potential of $K^+$ (usually around -90 $mV$).

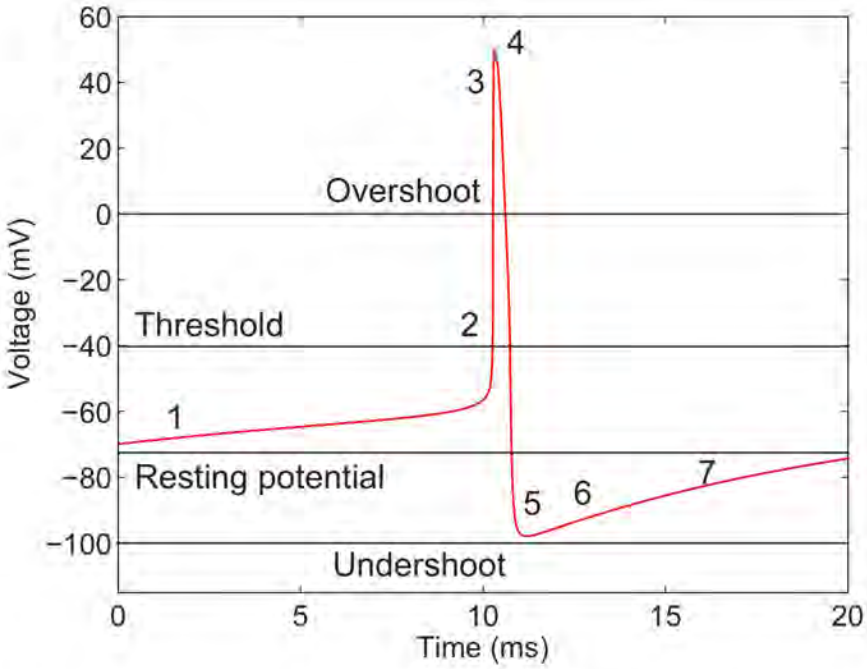


**Figure 2.2:** The action potential of a neuron. The typical trajectory of an action potential results from various membrane mechanisms: 1: weak depolarization, 2: fast depolarization, 3: repolarization, 4: inactivation of $Na^+$ channels, 5: deinactivation and closing of $Na^+$, 6: inactivation and closing of $K^+$ channels, 7: opening of inward rectifier $K^+$ channels. [ Purves et al., (2004) ]

4. **Inactivation of $Na^+$ channels:** The $Na^+$ channels become plugged from the intracellular side. During this about 1 $ms$ lasting time which is called *refractory period* no action potential can be initiated.

5. **Deinactivation and closing of $Na^+$ channels:** The Plug is removed and the channels close. The membrane potential falls below 0 $mV$ which is called *undershoot*.

6. **Inactivation and closing of $K^+$ channels:** The membrane potential is stabilized by the leakage of the ions.

7. **Opening of inward rectifier $K^+$ channels:** In this final step the membrane potential returns to the resting potential of the cell.

## 2.2 Electrophysiological Monitoring

A common approach for studying activities in brains is by recording a neuron's action potentials using electrophysiological methods. Electrophysiology enables us to investigate the electrical activities of neurons. In principal we can distinguish intracellular and extracellular recordings.

### Intracellular Recordings

For intracellular recordings a thin microelectrode consisting of a glass pipette and a silver chloride-coated silver wire are used. This micropipette is contacted with the cell membrane, which then leads to the formation of a high resistance seal (also called *gigaseal*) between the glass tip and the cell membrane and allows the study of the contacted neuron. In general we distinguish the following two types of intracellular recordings. [ Molleman, (2003) ]

- The **patch clamp technique** was invented by Erwin Neher and Bert Sakmann [ Neher and Sakmann, (1976) ]. A schematic diagram is shown in Fig. 2.3. There are different modes of patch clamp as described in [ Hilscher, (2012) ]. For the *whole-cell patch clamp* an intracellular microelectrode with a small tip diameter of usually a few micrometers filled with an electrolyte solution is used. After the cell was contacted with the micropipette the cell's membrane is ruptured by a gentle suction through the mouthpiece on the other end of the pipette. This is also called *patch* and allows the measurement of the intracellular voltage. The measured voltage is the potential difference between the intra- and the extracellular fluid which is contacted with a reference electrode. Thus, stable recordings of the membrane potential of different neurons are now feasible and single action potentials can be measured. The biggest disadvantage of this method is that the intracellular fluid of the cell mixes with the electrolyte solution inside the recording electrode which can lead to the dilution of essential components in the cytosol. [ Verkhratsky et al., (2006) ]

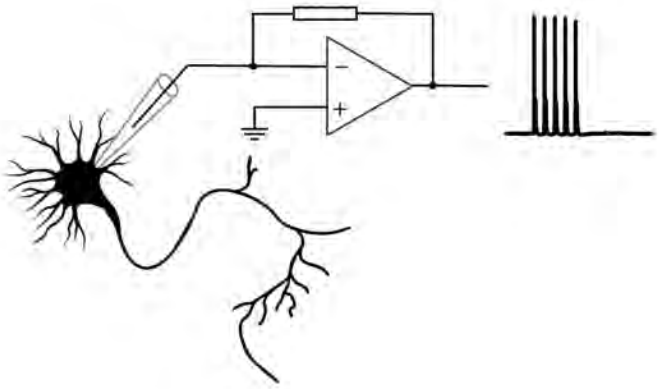


**Figure 2.3:** The patch clamp technique. This figure shows a schematic of the patch clamp technique, where a neuron is contacted with a pipette in order to measure the cell's activities.

- The **sharp electrode technique** is a method which uses a micropipette with a very small tip diameter in order to impale the cell's membrane. This results in a very little exchange of ions between the intracellular fluid and the solution in the pipette and allows to study the cell's properties. Nevertheless, since mechanical pressure is applied this method can harm the cells. Also, it does not allow as stable recordings as the patch clamp technique.

### Extracellular Recordings

A less invasive method for neuronal recordings is the extracellular recording. While intracellular recordings can result in a shorter lifetime of the contacted cells and also can cause the leakage of substances across the cell membrane since it is ruptured, extracellular recordings present a less damaging method. We can distinguish the following extracellular techniques [ Burns et al., (2010) ][ Buzsáki et al., (2012) ]:

- **Local field potential (LFP) recordings** are done by registering the activities of several cells. The microelectrode is placed a bit distant from a group of local neurons. Fig. 2.4 shows a schematic of the LFP technique. Usually a specific brain region is investigated and the potential of the present cells is measured. Thus, it can be difficult to distinguish the signals of single cells from "background noise". To get the LFP of the investigated cell group the signal usually is low-pass filtered afterwards. The process of assigning spikes to different neurons is called *spike sorting* which is one of the "hot topics" in computational neuroscience nowadays. [ Kajikawa et al., (2011) ]

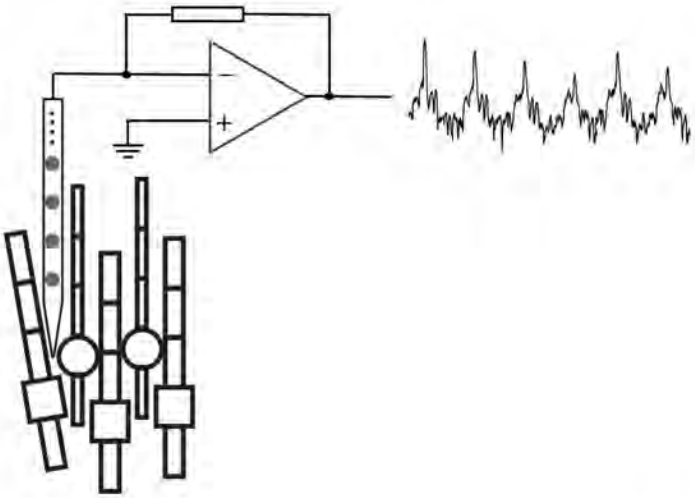

**Figure 2.4:** Local field potential recordings. This figure shows a schematic on how local field potential recordings are done. Therefore, a microelectrode is placed around a group of neurons in order to measure their collective activities.

- **Single / Multi unit recordings** can be done with a very thin microelectrode which is introduced into the brain or tissue. It is used to record the activities of single neurons or a small amount of cells depending on the glass pipette diameter. But in contrast to patch-clamp recordings, single unit recordings register action potentials of neurons with smaller amplitudes (in a range of about 1 $mV$ instead of the about 130 $mV$ range of recorded action potentials when patching neurons). [ Purves et al., (2004) ]

CHAPTER 3

# Optical Monitoring

Optical methods are the main subjects in this chapter. It presents the advantages of using optical approaches and introduces various microscopy techniques. Furthermore, it states devices needed for the digital capturing of images and discusses the tools needed in order to perform experiments with fluorescence emission. It also includes a short paragraph about the theoretical basics needed for light microscopy.

## 3.1 Microscopy

Since invasive approaches such as the patch clamp technique have some limitations and require a lot of precision in order to record from a specific neuron, microscopy techniques can be a very powerful support if not replacement in some cases. We distinguish three principal types of microscopy, namely *optical microscopy*, *electron microscopy* and *scanning probe microscopy*. While the latter two microscopy techniques are expensive to build and not practical for electrophysiological studies, optical microscopes are part of a standard electrophysiology setup.

Optical methods have the advantange of no or lower tissue damage since there is no impalement damage. Moreover, they have the ability of monitoring the spatial distribution of neuronal activity which is limited when recording with microelectrodes. Fluorescence microscopy for example, works for all neurons which are able to emit light or change light intensity in response to electrical or chemical changes of their membranes or in their environments and can be used to capture spatially separated neurons simultaneously and non-invasive. [ Tro, (2009) ][ Halliday et al., (2011) ]

Optical microscopy involves a light beam transmitted through or reflected from the sample under investigation. It uses lenses in order to mirror these beams and allows a magnified view of the sample. This results in an image which can be seen by eye or captured digitally. Digital capturing of images has very important aspects in neuroscience. These aspects range from the

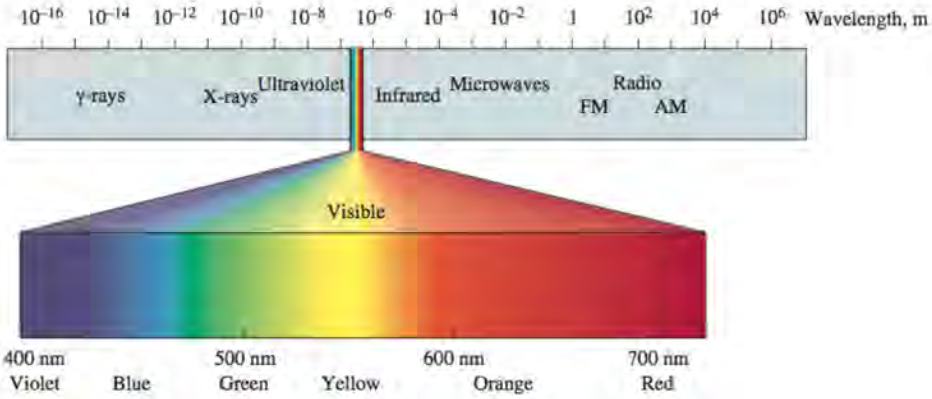


**Figure 3.1:** The electromagnetic spectrum. This figure shows the entire electromagnetic spectrum and a detailed view of the visible light. The illustration is taken from [ Tro, (2009) ].

documentation of experiments by life monitoring to the non-negligible possibility of recording light which can not be seen with the human eye. [ Ji et al., (2008) ]

Light is electromagnetic radiation which is visible for humans only in a specific wavelength range. This range extends from approximately 380 $nm$ to about 740 $nm$. Besides that, the electromagnetic radiation spectrum is grouped into *infrared*, *microwave* and *radio*, which have a longer wavelength than the visible light, and *ultraviolet*, *X-rays* and *gamma rays*, which have a shorter wavelength than the visible region. Wavelength is inversely proportional to frequency, meaning that shorter wavelengths have higher frequencies and longer wavelengths have lower frequencies.

Since, electromagnetic radiation consists of photons which have different energy levels, they are able to cause electronic excitation within molecules. This property is essential for all kinds of optogenetic tools where the excitation of a molecule changes its activity and conformation. For the human eye out of range are ultraviolet on one side of the spectrum, which has a range of range about 10 $nm$ to about 380 $nm$, and infrared on the other, which has a range of range about 740 $nm$ to approximately 1 $mm$ (see Fig. 3.1). While ultraviolet radiation is very harmful for cells and can damage their membranes very easily, red shifted light has become more and more important in neuroscience. Nowadays, there are a lot of different fluorescent dyes and indicators available which can monitor neuronal activities in up to far-red shifted or infrared wavelength ranges. An infrared signal can not be seen by the human eye though. Therefore, digital capturing, for example by a charge-coupled device (CCD) camera and monitoring on the computer screen is needed. [ Tro, (2009) ][ Halliday et al., (2011) ]

### Camera

In order to perform live-imaging of tissue, CCD cameras on microscopes are standard in electrophysiology setups nowadays. These cameras consist of a CCD image sensor whose pixels are p-doped metal–oxide–semiconductor capacitors. The term *p-doped* in this context means that the semiconductor contains excess holes, whereas an n-doped semiconductor contains excess free electrons. The capacitors allow the detection of light by the conversion of incoming photons into electron charges which can be read by the CCD. Alternatively, complementary metal-oxide-semiconductors (CMOS) based devices can be used, where each pixel contains a photodetector and an active amplifier, also known as *active-pixel sensor*. CCD cameras are better for weaker images, whereas CMOS cameras are mostly used for bright, strong fluorescence signals where the separation between strong and very strong fluorescence is needed.

### Microscopy Techniques

Since the contrast of living cells usually is too low for efficient optical recordings using standard approaches, different enhanced microscopy techniques have been invented in order to increase the contrast of the investigated samples. The most common ones, which are also existing as combinations, are the following ones [ Tro, (2009) ][ Halliday et al., (2011) ]:

- Bright field microscopy
- Oblique illumination microscopy
- Dark field microscopy
- Phase contrast microscopy
- Differential interference contrast microscopy
- Dispersion staining microscopy
- Confocal microscopy
- Interference reflection microscopy
- Differential interference contrast (DIC) microscopy
- Fluorescence microscopy

For our experiments we basically needed the benefits of the latter two microscopy techniques, which allow the imaging of living cells by either enhancing the contrast or monitoring stained tissue. Enhancing the contrast is very important when performing patch clamp experiments where the micropipette is lowered to the cellular level and contacted with the cell's membrane.

### Differential Interference Contrast Microscopy

DIC microscopy is an illumination technique which is used to enhance the contrast of unstained samples. Neurons usually have a low contrast because of their transparent appearance. DIC is very useful for neuronal cultures and thin tissue slices, where the samples under investigation and the background have a similar refractive index. The basic scheme of DIC microscopy is shown in Fig. 3.2. It is based on the separation of a polarized, in 45 degrees oscillating light into two parts which are aligned at 90 degrees to each other using a prism. The two rays are focused by the condenser lens and are passed through the sample. After passing the sample, the rays travel through the objective lens and are focused for a second prism. This second prism recombines the two rays again and polarizes at 135 degree which leads to interference and the formation of a signal with different amplitude and phase. This difference in amplitude and phase results from the difference in the optical path length which further leads to this typical three-dimensional optical image under very oblique illumination. A three-dimensional optical image makes it very pleasant to monitor tissue or cell cultures and living cells can be distinguished from surrounding tissue and dead cells very easily.

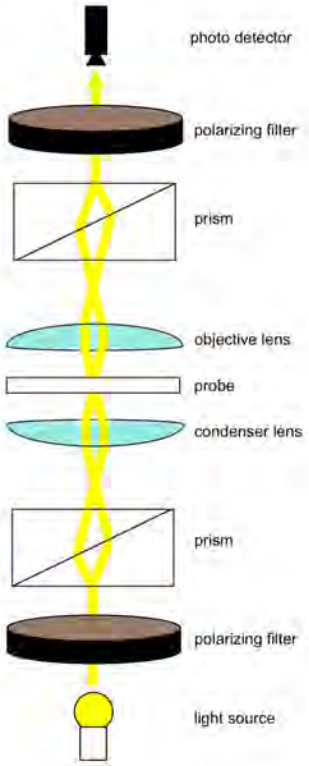


**Figure 3.2:** Differential interference contrast microscopy. This figure shows the way of light through a DIC microscope.

### Fluorescence Microscopy

This type of microscopy uses fluorescence, as the name suggests, in order to generate an image. This is important in many aspects. The most prominent one is that specific cells which are labeled using fluorescent markers can be detected. The sample under investigation, usually a piece of tissue or a neuronal culture, is illuminated with light of a specific wavelength which then is absorbed by fluorescent compounds of the cell, causing them to emit light of longer wavelengths. This emitted fluorescent light is "weaker" than the excitation, meaning that it has less energy but a higher wavelength. Therefore, a standard epifluorescence microscope as shown in Fig. 3.3, where excitation and observation are from above, usually consists of an excitation filter in order to filter the light with the right wavelength for the excitation of the probe and an emission filter in order to capture the emitted light from the probe. Furthermore, it normally has a dichroic mirror which acts like a bandpass filter and lets only a small wavelength range of light pass, while reflecting the rest. Thus, the dichroic beamsplitter lets light in a specific color pass, whereas reflects light in all the other colors. The light source on a fluorescent microscope can be a xenon arc lamp, a laser (Light Amplification by Stimulated Emission of Radiation), a high-power Light-emitting diode (LED) or a metal-halide lamp. While lasers are more commonly used for the stimulation of neurons in in vivo experiments, LEDs are sufficient enough for in vitro preparations. This is because lasers have a higher penetration depth and can be targeted more precisely than LEDs. Both, Lasers and LEDs usually have a certain wavelength range they are working in and have to be chosen very carefully.

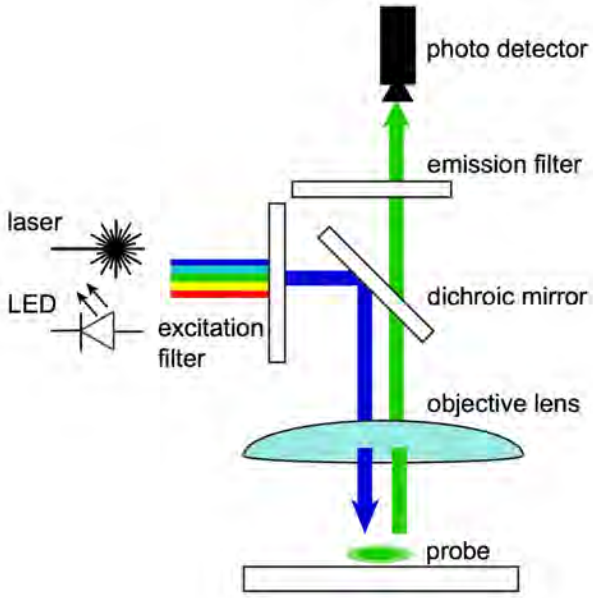


**Figure 3.3:** Fluorescence microscopy. This figure shows a schematic drawing of a fluorescence microscope, consisting of a light source, filters, a mirror, a lens, a detector and a probe.

The power of a laser usually is measured in light power ($mW$) or in light power per area ($mW/mm^2$). It is very important to know the diameter of the illuminated surface in order to use a laser with appropriate light power. Is the laser or LED too strong, the phenomenon of *photobleaching* can occur. This happens when the fluorescent compounds of the investigated cells undergo chemical damage because of electrons which are excited during fluorescence. Still the most efficient protection against photobleaching is to minimize the illumination, meaning that one should only turn on the fluorescence for the experiment. Also *phototoxicity* can have influential effects on the experiments. Mostly short wavelength light, like UV light can damage the cell membrane which then causes cell death. Nowadays, more stable fluorescent compounds are already available, but the side effects of the fluorescence light should always be kept in mind. [ Hell et al., (1994) ]

CHAPTER 4

# Fluorescent Probes

This chapter introduces to optogenetics, a technique which combines the advantages of optics and genetics in order to control the activity of individual neurons. It highlights the advantages and disadvantages of different optogenetical methods and provides a basic optogenetics-vocabulary for neuroscientists. This chapter also explains various fluorescent markers, such as fluorescent dyes, calcium indicators or voltage indicators and introduces the probes we used for our experiments.

## 4.1 Dyes

One of the first fluorescent techniques approaching neuroscience were dyes. Their usage has started already in the early 1960s, but because of their easy application they are still in use. Especially for the direct monitoring of electrical activities, dyes are very practicable. There are voltage-sensitive dyes (VSDs) and calcium-sensitive dyes which have different properties and dynamics. [ Canepari and Zecevic, (2010) ]

### Voltage-sensitive Dyes

This type of compound changes its light intensity or spectral properties in response to voltage changes which gives the dye its name. VSDs are lipophilic and bind to the cellular membranes [ Grinvald et al., (1982) ][ Grinvald and Hildesheim., (2004) ]. Normally they are applied extracellularly but can also be loaded internally by patching the cell. Due to the loading time, which is usually around 1 hour, the cell has to be patched twice, which makes this type of approach very unpractical. Furthermore, they can be toxic for living tissue since they can affect the properties of $K^+$ channels and synapses. However, VSDs provide signals as fast as the membrane potential time scale and reliable optical detection without the need of averaging [ Ferezou et al., (1998) ][ Bradley et al., (2009) ]. We can distinguish between two groups:

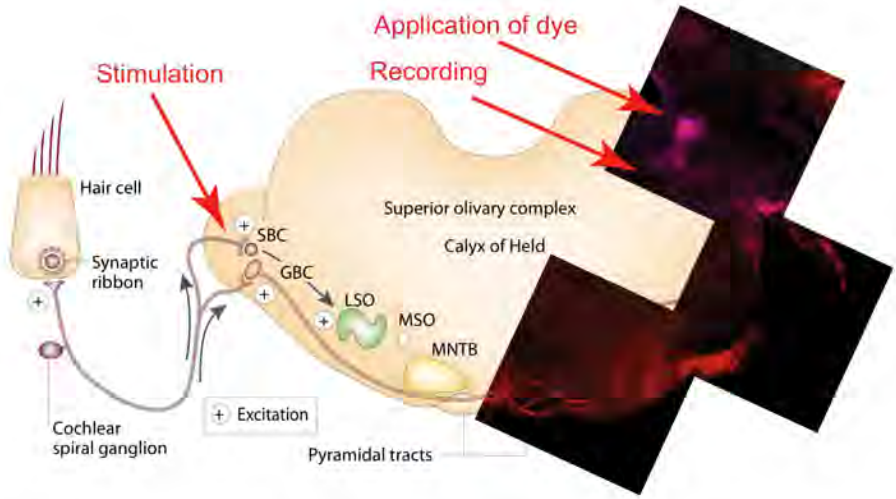


**Figure 4.1:** Voltage-sensitive dye. This figure shows a coronal section of the auditory brainstem from a tinnitus study where we applied the dye di-4-ANBDQPQ in order to monitor contralateral (other side) activities. The dye was applied in one spot (see arrow) and "travelled" to the dorsal cochlear nucleus. We optically recorded the voltage changes caused by inputs from the electrically stimulated contralateral dorsal cochlear nucleus. The illustration of the auditory brainstem circuitry is modified from [ Gersdorff and Borst, (2001) ]. VSD in pink, Chrna2+-cells (nicotinic acetylcholine receptor subtype alpha 2) in red. GBC/SBC-globular/spherical bushy cell, LSO/MSO-lateral/medial superior olive, MNTB-medial nucleus of the trapezoid body.

- **Slow dyes** are dyes, which respond to potential-dependent changes in the cell membrane in a range of milliseconds and are used to primarily measure "static" properties of cells, such as the resting potential. Their change in fluorescent is too slow in order to detect fast events such as APs of neurons. Typical examples of this dye are cyanine dyes. [ Wilson et al., (1985) ]

- **Fast dyes** on the other hand respond in microseconds, which makes them suitable for the recording of single APs. Nowadays, there are various voltage-sensitive dyes available. The most common used ones are aminonaphthylethenylpyridinium (ANEP) dyes such as, di-4-ANEPPS [ Fluhler et al., (1985) ][ Loew et al., (1992) ] or di-8-ANEPPS [ Bedlack et al., (1992) ][ Gross et al., (1994) ]. More specific ones are di-4-ANEPPDHQ [ Obaid et al., (2004) ], di-4-ANBDQPQ or di-4-ANBDQBS. All these dyes differ in the excitation wavelength, the emission wavelength, the exposure time, the voltage sensitivity and the response time which requires a lot of considerations and a very good considered selection. [ Canepari and Zecevic, (2010) ] Fig. 4.1 shows a picture of the deep-red dye di-4-ANBDQPQ applied on a coronal section of the auditory brainstem. This dye emits fluorescence in a spectrum not visible for the human eye. Therefore, confocal microscopy was done and the deep-red fluorescence (in pink) was imaged on a computer screen.

### Calcium-sensitive Dyes

The second major class of dyes includes calcium-sensitive dyes which register variations in $Ca^{2+}$ concentration. This type of dye can be used for the recording of both supra- and subthreshold events, such as synaptic inputs in individual dendritic spines, which are hardly reachable for electrophysiological methods. [ Svoboda et al., (1997) ][ Fetcho et al., (1998) ][ Maravall et al., (2000) ]. On the other side, calcium-sensitive dyes rely on the slow time course of the $Ca^{2+}$ dynamics, which means that the time scale is too slow for continuous action potential detection. An advanced approach is to combine voltage-sensitive dyes and calcium-sensitive dyes in order to simultaneously investigate action potentials together with synaptic inputs [ Berger et al., (2007) ][ Canepari and Zecevic, (2010) ][ Hagenston and Bading, (2011) ].

Although calcium-sensitive dyes have the advantage of being a non-invasive approach and making imagining of large cell groups possible, they have some notable drawbacks. One for example is the preparation itself, which can vary easily from one experiment to the other since the dye is applied extracellulary and "travels" from the injection site through connective tissue to the different cells until it binds to their membranes. Moreover, noise can be a problem when detecting the signal of specific cells, since the labeling of all cells in the tissue increases background noise and decreases the signal-to-noise ratio. Another issue is the high toxicity or photobleaching of organic dyes which does not allow experiments lasting longer than some hours. The most important limitation though, is the lack of neuronal selectivity. Dyes are not suitable for the marking of specific cell populations. Table 4.1 summarizes the advantages and disadvantages.

| Advantages | Disadvantages |
|---|---|
| Response of many active cells can be recorded | Not reporting specific populations |
| Can image small structures (e.g. dendritic spines) | Not reporting individual action potentials |
| Several options for filling the cells with the dye | Suprathreshold stimuli may be needed |
| Incubation with the dye is possible | Toxic effects |

**Table 4.1:** Advantages and disadvantages of dyes

### Intracellular Dyes

A more specific approach is to record the activity of individual neurons by patching single cells and filling the intracellular space with a dye through the pipette. This allows a more precise targeting of the dye and permits studies of electrophysiological properties as well as morphological characteristics. Loading not only one, but a few neurons in a defined region is also practical with this approach. A common example is the intracellular staining with biocytin. However, the micropipette through which the dye diffuses into the cell has to be removed after a certain time, otherwise the dye can diffuse back to the pipette. Another disadvantage is the limitation of studying electrophysiological and morphological properties at the same time, since the dye also needs some time to load and stabilize. This gives rise to another important optogenetical method, namely the engineering of fluorescent proteins.

## 4.2 Fluorescent Proteins

In the 1960s Osamu Shimomura started his studies in order to investigate where the glow of the jellyfish *Aequorea victoria* came from. He discovered and purified its luminescent proteins and named them *green fluorescent proteins* (GFPs) according to their expressing color [ Shimomura et al., (1962) ]. This simple green fluorescent protein should have a revolutionary impact on today's neuroscience. Suddenly there was a tool available which made it possible to genetically label different cell types, without the need of applying a dye. The remarkable property of this fluorescent protein is that the chromophore, which is responsible for the protein's color, does not require any cofactors or enzymes [ Tsien et al., (1998) ]. Especially this characteristic allows the introduction of GFP into a big variety of cells and even different species.

Nowadays, there are a lot of different mutations of the originally discovered protein available. All these FPs have stable excitation and emission spectra, optimized maturation at $37°C$, high protein stability and good resistance to pH variations. The peak excitation of GFP is at 488 $nm$, the peak emission at 509 $nm$. There is also a shifted version of the GFP called *enhanced GFP* (EGFP) which has its excitation peak at 485 $nm$ and its emission peak at 530 $nm$. The cyan fluorescent protein (CFP) and the yellow fluorescent protein (YFP) are mutations of the GFP as well. CFP has its excitation peak at 436 $nm$ and its emission peak is at 480 $nm$. YFP is best excitable at 514 $nm$ and emits light with 527 $nm$ peak-wavelength. Probably, the most prominent red fluorescent proteins because of their resistances to photobleaching are *mCherry* and *tdtomato*. The fluorescent protein tdtomato is six times brighter than EGFP and has its maximum excitation at 555 $nm$ and its emission wavelength at 581 $nm$ whereas mCherry has its excitation peak at 587 $nm$ and its emission maximum at 610 $nm$. The letter "m" in the name mCherry results from the abbreviation of *monomeric*, "td" in the name tdtomato stands for *tandem dimer*.[ Gautam et al., (2009) ][ Chudakov et al., (2010) ][ Dugué et al., (2012) ]

All FPs have one peak-value for the excitation wavelength and one peak-value for the emission wavelength. These values denote the wavelength where the protein is best excitable and the wavelength in which most of the emission occurs, respectively. In order to reach the best excitation frequency of the protein and also to capture most of the emitted light, filters for the precise alignment are used. Fig. 4.2 shows the excitation (dashed) and emission (solid) spectra of CFP, YFP and Alexa568 which is very similar to mCherry. [ Daya and Davidson, (2009) ]

One can see the peak excitation and peak emission wavelength of the aforementioned proteins. These peak-values are the ones which are usually named when talking about a specific fluorescent protein. Neuroscientists usually also name the appropriate filters on the microscope according to the protein. Green filters are usually called *GFP*, *Cy2*, *DiO* or *Alexa488*. Yellow filters are normally called *YFP*, *Cy3* or *Alexa546*, red ones are called *tomato*, *Cy5* or *Alexa568*. Capturing far-red fluorescence, the filters are typically named *deep-red* or *Alexa633*. The number after "Alexa" determines the wavelength of the excitation or emission. With the wrong excitation filter, the protein can be excited, but maybe too little in order to show any effect. The same is valid for the emission filter. Using the wrong filter, can result in the capturing of the wrong

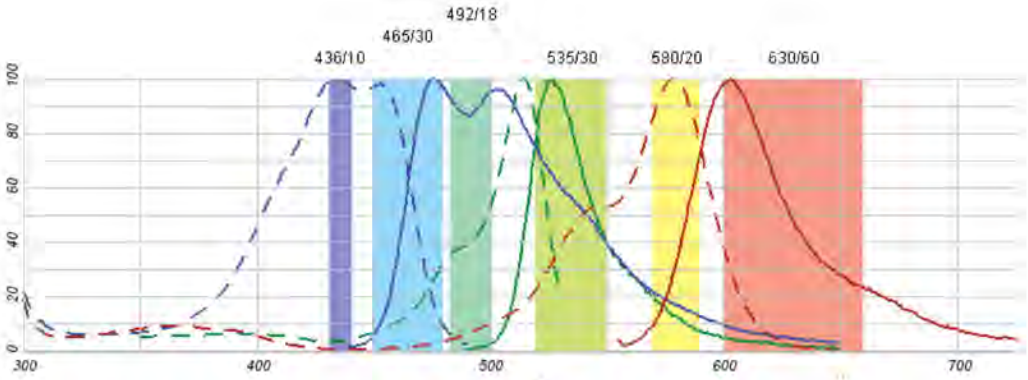


**Figure 4.2:** Excitation and emission spectra. This figure shows the excitation (dashed) and emission (solid) spectra of CFP, YFP and Alexa568 including different filters [ Martin, (2007) ].

wavelength. Also the light source, in particular the LED, should match the excitation spectrum of the protein under investigation. Usually only one fluorescent protein emission spectrum is recorded at the same time. For the capturing of different cell types with different fluorescence in one image, a series of single images is taken and combined to one image afterwards. For our experiments when testing three different fluorescent probes, we only needed one excitation filter and one emission filter at the same time.

### Fusion Proteins

However, the fluorescent protein alone is not the remarkable technique which is dominating neuroscience research these days. Nowadays, there are so-called *fusion proteins* available. Only the fusion of a fluorescent protein with a targeted protein allows the quantification of other proteins and as a consequence the investigation of whole cell activities. The first protein acts as a biosensor, which detects variations related to specific physiological signals such as $Ca^{2+}$ concentration, pH or voltage. Changes in these properties cause a conformational change in the sensor protein and yield the second protein, which is fluorescent, to convert the physiological changes into variations of fluorescence emission. Moreover, it is even feasible to optically image the activities of subcellular compartments of genetically identified cells. [ Knöpfel, (2012) ]

### Genetically Encoded Indicators

In order to record the aforementioned physiological variations by fluorescence change, both a high spatial and a high temporal resolution are needed for the study of neuronal activities. These requirements in general are fulfilled by fluorescent proteins, but especially the possibility of precise targeting makes the FPs so attractive compared to fluorescent dyes. Therefore, the fluorescent reporter protein just needs to be expressed by the neuron of interest. This is done by genetically introducing it to the neuron and expressing it under the control of a promoter using viral vectors, electroporation techniques or transgenic lines, which gives these proteins also the

name *genetically encoded indicators*.

Genetically encoded calcium indicators and genetically encoded voltage indicators are the most widely used GEIs in neuroscience nowadays [ Knöpfel et al., (2006) ][ Scanziani and Häusser, (2009) ]. They are generally composed of two fused proteins which are connected as follows:

- either a single FP is fused to a sensor domain by a short spacer, or
- two different FPs have their fluorescence emission paired, based on fluorescent resonance energy transfer (FRET).

### Fluorescent Resonance Energy Transfer

This mechanism is also called *Förster resonance energy transfer* and describes the energy transfer from a donor chromophore to an acceptor chromophore. The common name in literature is *fluorescence resonance energy transfer* though, especially when both chromophores are fluorescent. This can be misleading, since the energy is not transferred by fluorescence itself but between the chromophores. FRET is dependent on the distance between the two chromophores. The distance of the energy transfer is much smaller than the wavelength of the emitted light and typically between 10 and 100 Å (= between 1 and 10 $nm$). FRET only works, if the excitation spectrum of the acceptor overlaps with the fluorescence emission spectrum of the donor (see Fig. 4.3 A). In his studies, Förster showed that the "efficiency" $E$ of FRET depends on the inverse, to the power of six, distance between the donor and the acceptor (see Eqn. 4.1). [ Förster, (1948) ][ Held, (2006) ]

$$E = \frac{Ro^6}{Ro^6 + r^6} \tag{4.1}$$

In this equation *Ro* is the Förster radius in Å at which half of the energy is transferred and *r* denotes the distance between the donor and the acceptor molecule. The Förster distance (*Ro*) is shown in Eqn. 4.2 and depends on various factors, including the fluorescence quantum of the donor *fd*, the refractive index of the solution *n*, the angular orientation of each molecule $k^2$ and the spectral overlap integral of the donor and the acceptor *J*.

$$Ro = 9.78 * 10^3 (n^{-4} * fd * k^2 * J)^{\frac{1}{6}} \tag{4.2}$$

If *Ro* is set to 1 and the distance between the donor and the acceptor is also set to 1, Eqn. 4.1 turns into

$$E = \frac{1^6}{1^6 + 1^6} = 0.5 \tag{4.3}$$

which gives the value for the Förster distance where half of the energy is transferred. If the donor and the acceptor molecule are 10 times closer, meaning that

$$r = 0.1 * Ro \tag{4.4}$$

the FRET gets more efficient as seen in Eqn. 4.5

$$E = \frac{1^6}{1^6 + 0.1^6} = 0.999999 \tag{4.5}$$

If the donor and the acceptor molecule are 10 times more distant, meaning that

$$r = 10 * Ro \tag{4.6}$$

the FRET gets less efficient as seen in Eqn. 4.7

$$E = \frac{1^6}{1^6 + 10^6} = 0.000001 \tag{4.7}$$

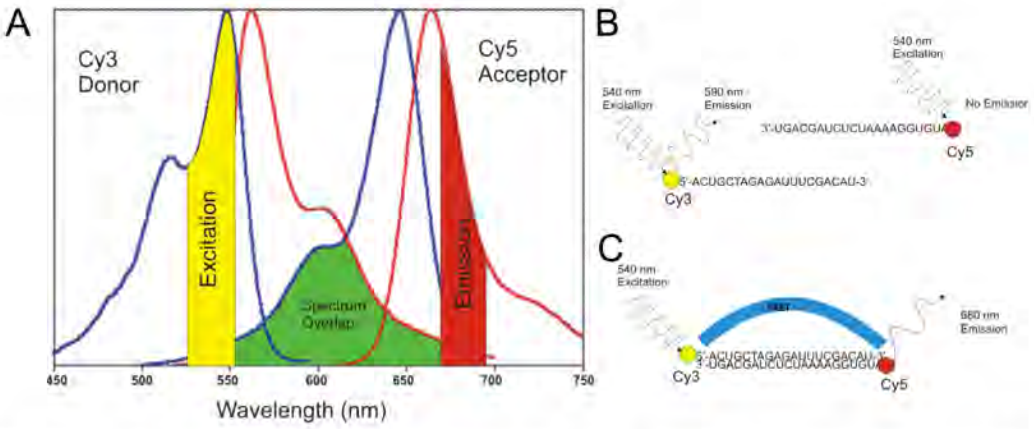


**Figure 4.3:** Fluorescent resonance energy transfer. A: The schematic representation of the spectral overlap of Cy3 (yellow) and Cy5 (red) is shown in green. B: A schematic drawing of two independent fluorescent molecules. C: A schematic drawing of FRET between two fluorescent molecules. The illustrations are taken from [ Held, (2006) ].

In neuroscience FRET is usually connected to a pair of fluorophores. A common FRET-pair is CFP as a donor molecule and YFP as an acceptor. But also Cy3 as a donor, emitting at maximally 590 $nm$ and Cy5 as an acceptor, emitting at maximally 680 $nm$ is a possible FRET-pair. Fig. 4.3 B shows how FRET for Cy3 and Cy5 could work. When the two molecules are not close enough, an excitation of Cy3 with light at 540 $nm$ results only in the emission of light by the Cy3 with 590 $nm$. The Cy5 does not emit any light, neither with 590 $nm$ nor with 670 $nm$. But, when the two molecules are within the Förster distance, FRET occurs. Exciting the Cy3 with light at 540 $nm$ results in the emission of light by the Cy5 with 680 $nm$. In other words, FRET causes a decrease of Cy3 fluorescence (not all of the emission at 590 $nm$ is lost) and an increase of Cy5 fluorescence. [ Held, (2006) ][ Taniguchi et al., (2007) ]

## 4.3 Voltage Indicators

One of the most prominent fluorescent proteins using FRET, is the *voltage-sensitive fluorescent protein*. This voltage indicator is able to detect changes in the cell's membrane potential and converts these changes into fluorescence signals. The fluorescence signals then correspond linearly to the changes of the cell's activities. These activities are usually expressed as action potentials or membrane potential changes due to synaptic inputs. VSFPs combine the advantages of voltage-sensitive dyes and genetically encoded indicators, meaning that they stay in the membrane of the neuron and rearrange their configuration dependent on variations in the voltage but are less toxic and faster than the dyes. Furthermore, they can be expressed by the neuron itself and do not need to be applied extracellularly. [ Knöpfel, (2012) ]

VSFPs are based on the voltage-sensitive domain of the voltage-sensitive phosphatase from the sea squirt *Ciona intestinalis* (Ci-VSP) [ Villalba-Galea et al., (2009) ]. The first attempts of using voltage-sensitive fluorescent proteins were:

- **FlaSh** which is a GFP attached to a $K^+$ channel (Kv1.4), and
- **SPARC** using a $Na^+$ channel (NaV1.4) with a fluorescent protein, yielding to the nowadays known VSFPs [ Canepari and Zecevic, (2010) ].

Thomas Knöpfel who is one of the pioneers in the research of voltage-sensitive fluorescent proteins and his collaborators engineered various types of VSFPs [ Dimitrov et al., (2007) ][ Mutoh et al., (2009) ][ Perron et al., (2009) ][ Akemann et al., (2012) ]:

- **VSFP1:** It is based on a voltage dependent $K^+$ channel and fused to a fluorescent protein pair, namely CFP and YFP [ Sakai et al., (2001) ]. Since it was one of the first developed VSFPs it has some limitations. Especially the targeting to the plasma membrane of mammalian cells, but also the optical imaging of APs is very limited [ Baker et al., (2008) ].
- **VSFP2:** This variant of VSFP is constructed of four-transmembrane voltage domains (S1-S4) which are connected to the fluorescent protein pair using FRET (see Fig. 4.4). The targeting to the plasma membrane of mammalian cells could be improved as reported in [ Akemann et al., (2010) ] and [ Knöpfel et al., (2010) ]. Although improved, the optical imaging of APs still needs averaging techniques of multiple trials.
- **VSFP2.3:** It was the first VSFP version permitting the optical imaging of action potentials in brain slices and allowed the imaging of APs without averaging of multiple trials [ Akemann et al., (2010) ].
- **VSFP3:** This VSFP uses a single fluorescent protein instead of FRET, which gives rise to faster kinetics and a broader color spectrum but a smaller signal amplitude compared to the predecessor versions. [ Perron et al., (2009) ]

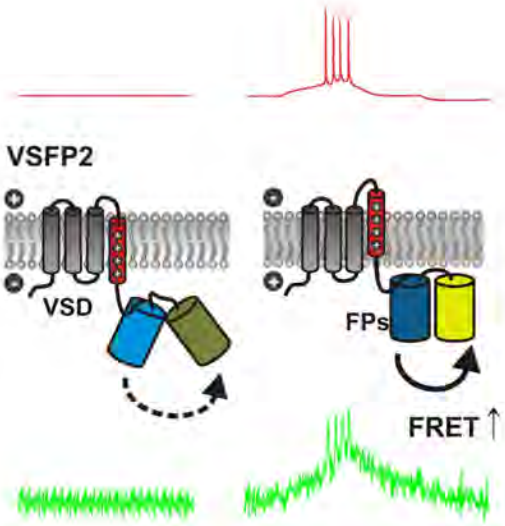


**Figure 4.4:** Monitoring using VSFP2. This figure shows the optical reporting of action potentials (red traces) by VSFP2 (green traces) using FRET. [ Knöpfel et al., (2010) ]

The state-of-the-art approach is the so-called *VSFP-butterfly* which combines the properties of VSFP2 (good targeting to the plasma membrane) and VSFP3 (faster kinetics and broader color spectrum). In this version of VSFP the voltage sensor, which detects the membrane changes, is placed between two fluorescent proteins. The two FPs use FRET in order to report conformation changes by fluorescence emission. VSFP-butterflies can be targeted very well to the cell membrane and have already been shown to report subthreshold oscillations [ Akemann et al., (2012) ][ Perron et al., (2012) ]. Two VSFP-butterflies should be mentioned here:

- **VSFP-butterfly1.0:** This version of VSFP is composed of the two fluorescent proteins *mCerulean* and *mCitrine*. The excitation peak of mCerulean is 458 $nm$, the emission 490 $nm$, meaning that it is a blue shifted fluorescent protein. The FP mCitrine on the other hand is a yellow fluorescent protein with its excitation peak at 516 $nm$ and its emission peak at 529 $nm$. The problem of the VSFP-butterfly1.0 is still the relatively small SNR when detecting membrane potential changes.
- **VSFP-butterfly1.2:** It consists of the two fluorescent proteins *mCitrine* and *mKate2*. Here mCitrine is the donor protein and mKate2 the acceptor, which is the newer version of the far-red fluorescent protein TagFP635 (also known as mKate). It has its excitation peak at 588 $nm$ and its emission is at 594 $nm$. [ Shcherbo et al., (2007) ][ Shcherbo et al., (2009) ] The VSFP-butterfly1.2 has a good SNR which makes the fluorescence signal easier detectable. Furthermore, it has a high photostability and low cytotoxicity. In this study we expressed the VSFP-butterfly1.2 in cultures and compared its potential in detecting action potentials and synaptic inputs with genetically encoded calcium indicators.

## 4.4 Calcium Indicators

While voltage indicators monitor the voltage change of a cell's membrane, calcium indicators monitor changes in $Ca^{2+}$ concentration. They are composed of a FP fused with a $Ca^{2+}$-binding domain. There are two principal groups of GECIs. [ McCombs and Palmer, (2008) ]

The first group contains indicators comprised of the $Ca^{2+}$–sensitive protein *calmodulin* (CaM) linked to either a single fluorescent protein (e.g. GCaMP, GECO) or a FRET-based pair of FPs (e.g. the protein *yellow cameleon*). [ Tian et al., (2009) ] [ Horikawa et al., (2010) ][ Zhao et al., (2011) ][ Akerboom et al., (2012) ]

The second group contains indicators consisting of the protein *troponin C*. This protein is expressed in muscle cells and it is believed that it reduces interactions with $Ca^{2+}$-sensing targets compared to CaM, which is very important when detecting membrane potential variations through changes in calcium concentration since there is no interference with the measured signal. [ Canepari et al., (2008) ][ Mank and Griesbeck., (2008) ]

Examples of genetically encoded calcium indicators are:

- **Cameleon**, which is based on GFP variants and CaM - it uses FRET for the monitoring of calcium changes;
- **D3cpV**, which is also a calmodulin based FRET sensor - with this GECI it is possible to detect single APs;
- **YC3.60**, which stands for a version of the protein yellow cameleon and is able to detect bursts with up to 10 APs;
- **TN-XXL**, which is a troponin C based indicator - it allows the chronic $Ca^{2+}$ imaging in flies and mice;
- **GCaMP**, which uses a single fluorescent protein - it is a fusion between GFP, Calmodulin and the peptide M13 (see Fig. 4.5). M13 is a "conformational actuator" and part of the myosin light chain kinase which can bind CaM. It enhances conformational changes and fluorescence modulation. Similarly to VSFPs, there have been various versions of the GCaMP engineered. With GCaMP3 it was possible to detect when APs occurred, but since the kinetics of this calcium indicator are very slow, it does not seem to have the possibility of reliably detecting single APs. This was first possible with GCaMP5 [ Akerboom et al., (2012) ].
- **R-GECO1** (red-genetically encoded $Ca^{2+}$ optical indicator 1), which is a red-shifted GECI, based on the substitution of the GFP by the far-red shifted protein *mApple* (excitation: 568 $nm$, emission: 624 $nm$) [ Zhao et al., (2011) ].

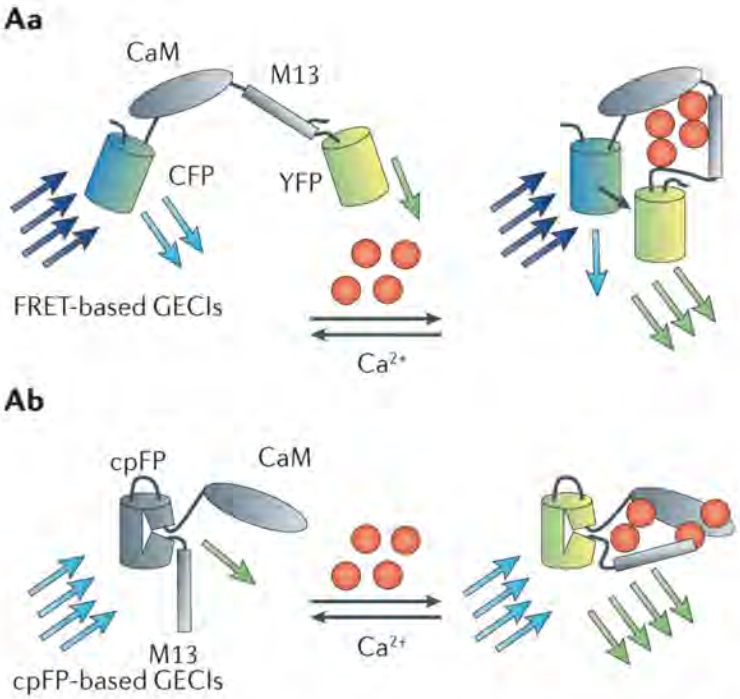


**Figure 4.5:** Monitoring using GECI. This figure shows a schematic drawing of calcium indicators. Aa: FRET-based calcium indicators often use CFP and YFP. The excitation of CFP with 440 $nm$ light (blue arrows) results in cyan (cyan arrows) and yellow (yellow-green arrows) FRET fluorescence. Binding of $Ca^{2+}$ (red filled circles) to a calcium-binding domain (such as the CaM-M13 complex) increases the efficacy of FRET between CFP and YFP. Ab: Single fluorescent protein indicators incorporate a circularly permuted fluorescent protein (cpFP). The binding of $Ca^{2+}$ to the CaM-M13 complex increases the cpFP fluorescence. [ Knöpfel, (2012) ]

In our study we expressed GCaMP3 and R-GECO1 in cultures and compared them with the VSFP-butterfly1.2 in order to quantify how good these different proteins could report action potentials and synaptic inputs by their fluorescence emission. The ultimate goal for further studies is to express these fluorescent proteins in animal models after the expression and detection was promising in cell cultures.

# CHAPTER 5

# Cell Cultures

This chapter explains the great benefits of working with cell cultures, rather than with animal models. Besides showing a description on how to make cultures, it also includes a protocol on how to get DNA from plasmids and how to transfect the cultured cells. Furthermore, it includes a section which introduces a hybrid approach in order to investigate if the transfection caused any conformational changes in the cells and shows how to test if the GEIs worked properly.

## 5.1 Why Cell Cultures?

Nowadays, there are a lot of different techniques available in neuroscience, ranging from in vivo experiments to in vitro preparations. Cell cultures are used in order to grow cells under controlled conditions in vitro. Isolated from their normal biological surroundings, these cells can be grown and treated easier than in their natural environment, which is usually living tissue. One can imagine that there are thousands of cells and thus millions of proteins, molecules and genes present in such a living tissue. A hippocampal slice for example has plenty of cells interacting with one another. This interaction is very complex, reaching from simple molecule exchange to more complex signaling mechanisms influenced by temperature, light, sound, pH and so on. Cell cultures usually maintain these environmental parameters, but on a more comprehensible level and a smaller number of elements, which makes them very attractive for neuroscientists. On the other hand, there are some limitations though which are not relevant when studying a cell in its natural environment. Once the organism of the cell culture is working, the question is how much the results can be extrapolated from the culture to the intact organism, such as the brain. Also the effects of specific neuronal processes are not so easily predictable. A drug for example can work very well in the culture, but can have toxic effects on other cells, which are not present in the culture but in the living organism. [ Doering et al., (2012) ] The same question is legitimate for our three fluorescent proteins. Nevertheless, hippocampal cultures gave us the great possibility to study the performances of the three proteins GCaMP3, R-GECO1 and VSFP-butterfly1.2 under controlled and similar conditions.

There are different ways of cell culture preparations. One of the most common ones is a plasmid preparation, where plasmid deoxyribonucleic acid (DNA) is extracted, purified and introduced to the cells. We used plasmids carrying complementary DNA (cDNA) for GCaMP3 (Addgene plasmid Nr.22692), for R-GECO1 (Addgene plasmid Nr.32444) and for VSFP-butterfly1.2, which we obtained from Thomas Knöpfels laboratory.

## 5.2 DNA Preparation

Complementary DNA is used to clone genes from one type of cell in another, different cell. In order to express a specific protein, the cDNA that codes for this protein is transferred to the cell. This cell naturally does not express that protein. The cDNA which is introduced, is DNA synthesized from a messenger ribonucleic acid (mRNA), more precisely, it is a complementary copy of the mRNA, which is translated into a protein afterwards. Complementary DNA is an intron-free mRNA, which is needed for the expression of eukaryotic (cells with nucleus) genes in prokaryotic cells (cells without membrane-bond nucleus). Introns are nucleotide sequences, which are not coding sequences. This means, that the non-coding parts (introns) are cut out in order to make the translation into a protein possible. To achieve the right expression of a protein encoded by cDNA, also a promoter is required. Our plasmids were controlled by the CMV-promoter (*cytomegalovirus*), a strong promoter for gene expression in hippocampal cultures.

### DNA Purification

DNA purification is a procedure in order to extract and collect DNA. Mostly, plasmids are purified from bacterial cultures, typically *Escherichia coli* (E. coli). For our experiments, the Bacteria *DH5 alpha*, a strain of E. coli, was transformed with each of the plasmid vectors by heat shock and grown overnight at $37°C$ on agarose plates. Plasmids used in genetic engineering are also called *vectors*. These vectors carry genetic material originating from other cells into the target cell and encode one or more genes as a marker. We used 10 $\mu g/ml$ of the selectable marker ampicillin for VSFP-butterfly1.2 and R-GECO1, and 50 $\mu g/ml$ of the selectable marker kanamicin for GCaMP3 in our experiments. For the purification of plasmid DNA preparation kits are available. These kits are named by the size of the bacterial culture, called *miniprep*, *midiprep*, *maxiprep*, *megaprep* and *gigaprep*. Scientists also often give the extracted plasmid DNA the name of the *prep*, according to the kit it was performed in. We picked our plasmid DNA and amplified the E. coli culture in 250 $ml$ (maxiprep) of standard Lysogeny broth medium with 1 % ampicillin or kanamycin with overnight shaking at $32°C$.

In our experimental setup, DNA was purified using HiPure Plasmid Purification Systems (Invitrogen Nr.K2100-07). For the measurement of concentration and purity of the vectors a NanoDrop Spectrophotometer was used. As a control, the plasmids went through a polymerase chain reaction with specific primers, to verify their integrity. The GCaMP3, R-GECO1 and VSFP-butterfly1.2 plasmids then were ready to be introduced into the cell cultures. Since the preparation of neuronal cultures requires a lot of time and experience, we made some HEK cell cultures first in which we tested the expression and function of the three proteins.

## 5.3 HEK Cells

Human Embryonic Kidney (HEK) 293 cells are cells which are very easy to grow and can be transfected very nicely. They are called HEK cells since they were first obtained in human embryonic kidney cultures, the number 293 in the name originates from the number of the experiment. However, these cells are not neurons and are used in experiments where the activities of the cells are not of big interest, but the transfection and the expression of a protein for example. [ Doering et al., (2012) ] Thus, they were very useful for us to study the expression of our three fluorescent proteins.

Our HEK293 cells were grown in Dulbecco's Modified Eagle Medium (DMEM), composed of high glucose DMEM (Invitrogen Nr.11965-092) with 10 % Fetal Bovine Serum (Invitrogen Nr.16000-044) and 1 % PEST (100 $units/ml$ Penicillin + 100 $mg/ml$ Streptomycin; Invitrogen Nr.15140-148) at $37°C$ and 5 % $CO_2$. DMEM is a variant of Eagle's Minimum Essential Medium (EMEM) which is a cell culture medium used to maintain cells in tissue culture. DMEM is a liquid supporting cell growth and contains more vitamins and amino acids than EMEM. Since the medium is very important for cell cultures, it was passed two days before transfection and changed to RPMI-1640 serum free medium (Invitrogen Nr.22400-105) a few hours before transfection. We transfected our HEK cells with the plasmids using the TrueFect-Lipo kit (United BioSystems Nr.TF1101-1).

### Expression Analysis

48 hours after transfection, some HEK cells were fixed with 4 % formaldehyde for 10 $min$ in room temperature and then stained with DAPI (1:1000) for 10 $min$, in order to mark their nuclei. Coverslips with cells were washed with phosphate buffered saline, a buffer for immunohistochemical staining, before mounting to glass slides using mowiol mounting medium (see Fig. 5.1).

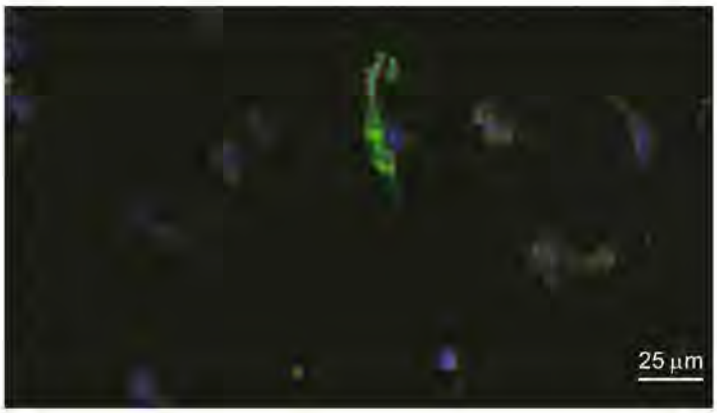


**Figure 5.1:** HEK cells expressing VSFP. This figure shows the fluorescence image (for mCitrine in green) of HEK 293 cells expressing VSFP-butterfly1.2 with nuclei labeled with DAPI (blue).

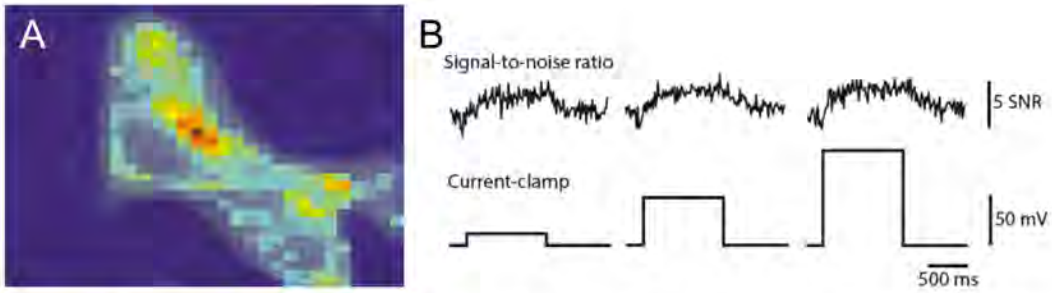


**Figure 5.2:** Optical and electrical signals of VSFP in HEK cells. A: This figure shows the fluorescence signal of a patched HEK cell expressing VSFP. B: The Signal-to-noise ratio values correspond to the membrane depolarizations, evoked by current injections.

### Electrophysiological Analysis

The major part of the transfected cells were plated on cover slips coated with poly-L-lysine (Sigma Nr.P2636) in order to perform electrophysiological recordings and fluorescence studies. Current-clamp recordings were done to optimize the set of excitation and emission filters as well as the best configuration for the data acquisition. Since we observed a response in fluorescence due to the change of the HEK cell's membrane potential, we further tried to detect evoked APs. Therefore, we simulated sodium, potassium and leak currents on a real-time computer and fed them back into the patched HEK cell, in order to pretend it was a neuron (see Fig. 5.2).

We used a biophysically realistic single compartment model of a basket cell, implemented as described in [ Wang and Buzsáki, (1996) ]. The spike-generating voltage-dependent ion currents ($I_{Na}$ and $I_K$) are based on the Hodgkin–Huxley equations [ Hodgkin and Huxley, (1952) ]. These equations form a mathematical model that describes the biophysical properties of a neuron and how action potentials are initiated and propagated.

$$C\frac{dV}{dt} = -I_{Na} - I_K - I_{Na} \tag{5.1}$$

with

$$I_{Na} = g_{Na} m_\infty (V)^3 h (V - V_{Na}) \tag{5.2}$$

$$I_K = g_K n^4 (V - V_K) \tag{5.3}$$

$$I_L = g_L (V - V_L) \tag{5.4}$$

including

$$m_\infty = \frac{\alpha_m}{\alpha_m + \beta_m} \tag{5.5}$$

$$\frac{dh}{dt} = (\alpha_h (1 - h) - \beta_h h) k \tag{5.6}$$

$$\frac{dn}{dt} = (\alpha_n (1 - n) - \beta_n n) k \tag{5.7}$$

In the equations 5.1 - 5.7, the letters *C, V, $V_{Na}$, $V_K$, $V_L$, t, $g_{Na}$, $g_K$, $g_L$, $I_{Na}$, $I_K$, $I_L$* and *k* describe capacitance density ($\mu F/cm^2$), transmembrane voltage ($mV$), reversal potential of $Na^+$ ($mV$), reversal potential of $K^+$ ($mV$), reversal potential of leakage ($mV$), time ($ms$), conductance density of $Na^+$ ($mS/cm^2$), conductance density of $K^+$ ($mS/cm^2$), conductance density of leakage ($mS/cm^2$), current density of $Na^+$ ($\mu A/cm^2$), current density of $K^+$ ($\mu A/cm^2$), current density of leakage ($\mu A/cm^2$) and a temperature coefficient for $21°C$ respectively. The parameters are C = 1, $g_{Na}$ = 35, $g_K$ = 9, $g_L$ = 0.1, $V_{Na}$ = 55, $V_K$ = -90, $V_L$ = -65 and k = 5.

The rate functions $\alpha_x$ and $\beta_x$ for *x = m, h* and *n* are calculated as follows. The three variables m, n, and h are the so-called *gating variables*.

$$\alpha_m = \frac{-0.1(V+35)}{exp(-0.1(V+35))-1} \tag{5.8}$$

$$\beta_m = 4\ exp(-(V+60)/18) \tag{5.9}$$

$$\alpha_h = 0.07\ exp(-(V+58)/20) \tag{5.10}$$

$$\beta_h = \frac{1}{exp(-0.1(V+28))+1} \tag{5.11}$$

$$\alpha_n = \frac{-0.01(V+34)}{exp(-0.1(V+34))-1} \tag{5.12}$$

$$\beta_n = 0.125\ exp(-(V+44)/80) \tag{5.13}$$

The model was implemented in the programming language C and solved in real time using the Euler method or the 4th order Runge-Kutta method (with a dt=0.05ms) on a computer running Linux and the Real Time Application Interface (RTAI) from the Politecnico di Milano Institute-Dipartimento di Ingegneria Aerospaziale (Mantegazza, http://www.rtai.org/). Inputs to and outputs from the model were acquired from the '10Vm' output and the 'command' input of the patch amplifier as previously described in [ Leão et al., (2009) ]. Here, the membrane voltage of the patched cell was read by the computer (V) and the ionic currents consisting of a sodium ($I_{Na}$, blue), a potassium ($I_K$, red) and a leakage ($I_L$ black) current (see Fig. 5.3 A) were continuously applied to the cell. This resulted in action potential like trajectories (see Fig. 5.3 B) when additionally depolarizing the cell through the current clamp amplifier with 10 $Hz$ current pulses. Our recording setup could also detect fluorescence changes due to the depolarizations in the cells, which allowed us to optimize our setup and continue with the transfection of the fluorescent proteins in real neurons.

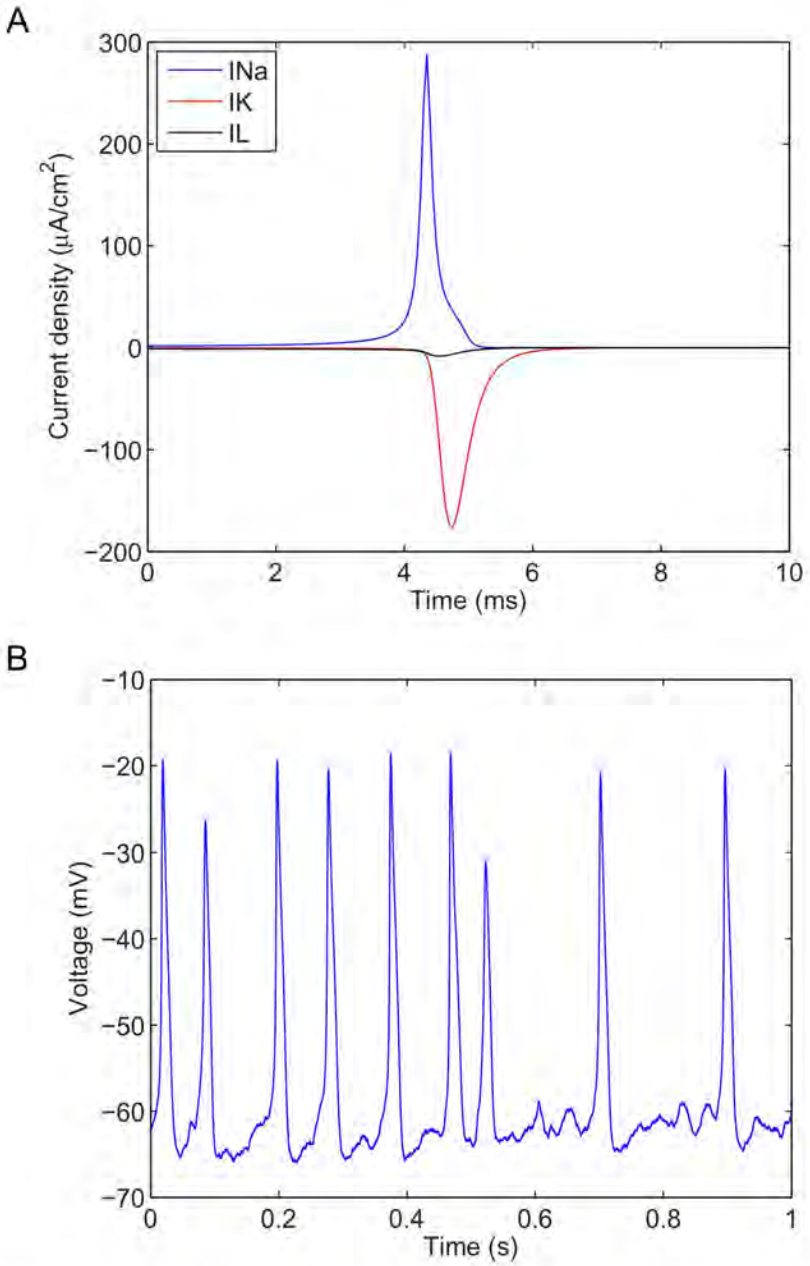


**Figure 5.3:** Ionic currents in a HEK cell. A: Simulation of sodium (blue), potassium (red) and leakage (black) currents of a basket cell, which were introduced to the patched HEK cells in order to pretend they were neurons. B: The membrane potential of a HEK cell when introducing the simulated ionic currents from A. Stimulation: 10 $Hz$.

CHAPTER 6

# Primary Hippocampal Neuron Cultures

This chapter describes how to obtain primary cultures of hippocampal neurons. It also explains how the cultures can be transfected with various genetically encoded indicators and prepared for the recordings. Therefore, the following paragraphs include a *standard operating procedure*.

## Experimental Approach

Since the final goal was to evaluate the expression of the three fluorescent proteins GCaMP3, R-GECO1 and VSFP-butterfly1.2 in nerve cells, primary cultures of neurons were made. Primary cultures consist of cells which were cultured directly from a biological environment, in our case from the hippocampus. The hippocampal neurons were obtained from P0-P2 (postnatal day 0 to postnatal day 2) mouse pups and isolated, dissociated and transfected. Afterwards they were carefully plated on cover slips in order to perform the expression studies of the three fluorescent proteins. Fig. 6.1 summarizes the design of our experiments.

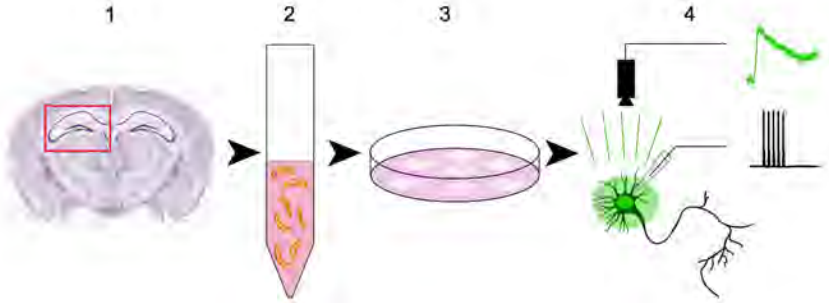


**Figure 6.1:** Experimental approach. This schematic drawing shows the experimental design. 1: Isolation of the hippocampi, 2: Dissociation and Transfection, 3: Culturing, 4: Recordings.

### Preparation of Tools

Before the hippocampi can be isolated, all the tools should be sterilized by spraying down the culture hood with 70 % of ethanol. The clean instruments then can be placed inside the hood. These tools are needed:

- sterile petri dishes which usually have a size of 6 or 10 $cm$
- sterile Poly-L-coated glass cover slips
- clean pipetters and tips

The following solutions which can be stored in a fridge at $4°C$ are needed as well:

- Dulbecco's Modified Eagle's Medium (DMEM)
- Neurobasal
- Phosphate buffer saline (PBS)
- Borate Buffer Solution
- Sodium Pyrovate Solution
- Sterile-filtered 20 percent Glucose Solution in distilled water

Furthermore, the following solutions which are stored in a freezer at $-20°C$ should be heated up in a waterbath at $37°C$:

- 5 $ml$ of horse serum
- 1 $ml$ of B-27 supplement
- 1 $ml$ of 100x antibiotics including penicillin plus streptomycin (PEST)
- 0.5 $ml$ of L-glutamine

As a last step, a 15 $ml$ conical tube should to be filled with 3 $ml$ PBS (10 $mM$) in order to collect the isolated hippocampi. [ Nunez, (2008) ][ Doering et al., (2012) ]

### Isolation of Hippocampi

For the isolation of the hippocampi, p0-p2 new born mice pups are needed. Right after they were euthanized, their heads need to be removed from the body and the skin needs to be cut away with scissors in order to open the skull. Using fine tweezers, the skull can be put away and the brain can be placed into a petri dish containing a small amount of PBS.

Having the brain placed in the petri dish, the hemispheres can be pealed back in order to reach the medial temporal lobe where the hippocampus is placed. The hippocampus looks like a small seahorse-shaped structure. Cutting around the nucleus with forceps removes connective tissue and isolates the hippocampus. (Step 1 in Fig. 6.1)

The same procedure needs to be done for the second hippocampus (since it is a bilateral structure) and for all the other pups in order to obtain more cultures. The hippocampi can be placed in the PBS-containing 15 $ml$ tube. [ Nunez, (2008) ][ Doering et al., (2012) ] (Step 2 in Fig. 6.1)

### Dissociation of Hippocampi

After all hippocampi have been isolated, the 15 $ml$ tube needs to be filled with 4.5 $ml$ PBS and 0.5 $ml$ of trypsin (Invitrogen Nr.25300-054). Trypsin is a digestion solution. The tube should be incubated for 15 $min$ to 30 $min$ at 37$°C$ before removing the PBS solution from the tube. This step should be done very carefully in order to not destroy the hippocampi that should have settled to the bottom of the tube. Another 5 $ml$ of PBS need to be added to the tube which then is incubated at 37$°C$ for 5 $min$. The step of removing the old PBS and replacing it with fresh PBS, is repeated twice.

Now, 0.5 $ml$ of DNase are added to the hippocampi in 4.5 $ml$ PBS. This DNase is added to promote enzyme activation. To make it homogenous, it has to be triturated (pipetting up and down without introducing bubbles) for a while.

Next, the cell viability should be determined using the trypan blue exclusion method. [ Nunez, (2008) ][ Doering et al., (2012) ]

### Transfection of the Cells

Now, the neurons should be centrifuged for 5 $min$ with 300 $rpm$, resuspended with 100 $\mu l$ of the Mouse Neuron Nucleofector Solution (Lonza Nr.VPG-1001) and mixed with 2-3 $\mu g$ of DNA of the GCaMP3, R-GECO1 or VSFP-butterfly1.2. For the transfection we used the Nucleofector from Amaxa Nucleofector Technology.

Nucleofection is a transfection method using electroporation in order to transfer DNA into the cell nucleus and the cytoplasm. Electroporation causes an increase of the permeability of the cell's membrane by an externally applied electrical field and thus allows the introduction of DNA into the cell. [ Doering et al., (2012) ]

### Preparation of Culture Plates

The last step in the protocol is to prepare the coverslips. Therefore, a 24-well cell culture plate (1 $ml$/well), containing cover slips precoated with both poly-L-lysine and laminin (Sigma Nr.L2020) after dilution with glucose DMEM, should be prepared. These are the coverslips, where the neurons are placed by pipetting the desired amount of cells to the petri dish. A gently swirling distributes the cells. [ Nunez, (2008) ][ Doering et al., (2012) ] (Step 3 in Fig. 6.1)

After the cells attached for 2 to 4 hours in a humidified, $37°C$ incubation chamber with 5 % $CO_2$, the coverslips can be tranferred to individual dishes containing Neurobasal medium (Invitrogen Nr.21103-049), supplemented with 2% B27 (Invitrogen Nr.17504-044), 2 $mM$ GlutaMAX (Invitrogen Nr.35050-061) and 1x PEST. The dishes should also be kept in the incubator and one-third of the medium should weekly be replaced with fresh Neurobasal medium.

### Imaging Hippocampal Neurons

The cultures should be maintained at $37°C$ in 5% $CO_2$. When the cultured hippocampal neurons have been in vitro for at least 48 hours, they should already have begun to form projections.

For our experiments, some cultures were fixed and immunocytochemistry protocols were applied in order to investigate their maturity for electrophysiological experiments. After 13 days in vitro (DIV) they showed the presence of MAP-2 and synapsin I, which were present in the axonal terminals (an indication for neuronal functioning) and allowed us to perform our recordings (Step 4 in Fig. 6.1). [ Nunez, (2008) ][ Doering et al., (2012) ]

CHAPTER 7

# The Experimental Setup

This work includes both experimental approaches as well as analytical methods in order to detect neuronal activities from the fluorescence signal of various proteins. Therefore, it is very important to plan such experiments and choose the appropriate materials and methods. This chapter provides the experimental protocols for the electrophysiological recordings as well as information about the optical setup we used. Furthermore, it contains a description on how we calculated if any fluorescence change happened caused due to APs occurring in the neuron.

## 7.1 Electrophysiological Recordings

Intracellular whole-cell patch clamp was performed on the transfected neurons which were transferred to a recording chamber. This chamber was perfused with external solution at room temperature (1 – 1.25 $ml/min$) containing (in mM) 120 NaCl, 3 KCl, 1.2 $MgCl_2$, 2.5 $CaCl_2$, 23 $NaHCO_3$, 5 HEPES, and 11 Glucose. Osmolarity was 300, pH 7.4 and adjusted with NaOH (1 M) if necessary. We used an Olympus microscope (BX50), equipped with a water immersion 40x objective (Nikon, NA 0.8). Recordings were done using a Dagan BVC 700A amplifier (Dagan Corporation, Minneapolis, USA) and data was acquired using a 16-bit data acquisition card (National Instruments) and WinWCP and WinEDR softwares implemented by Dr. J. Dempster (University of Strathclyde, Glasgow, UK). Patch-pipettes of borosilicate glass capillaries (GC150F-10 Harvard Apparatus) were pulled on a vertical puller (Narishige, Japan) with resistances around 7 $M\Omega$. Pipettes were filled with internal solution (~290 Osm) containing (in mM) 130 $K^+$-gluconate, 7 NaCl , 0.1 EGTA, 0.3 $MgCl_2$, 0.8 $CaCl_2$, 2 Mg-ATP, 0.5 Na-GTP, 10 HEPES, and 2 EGTA (pH was adjusted to 7.2 using KOH (1 M). Somatic current injections (400 $pA$, 1 $ms$) were applied through the patch-pipette, at frequencies ranging from 0.7 to 10 $Hz$.

## 7.2 Optical Recordings

Image series were acquired by an Andor DU-860 electron multiplying charge-coupled device camera (Andor, Belfast, Ireland). Fluorescence excitation was applied using a computer-controlled 200 $W$ metal-halide lamp (Prior Scientific). The electrophysiology rig was surrounded by black curtains and the CCD sensor of the camera was cooled to $-80°C$. The number of frames for the fluorescence recordings was calculated for each cell, based on the speed of the camera (~1000 frames per second) and the exposure (time of light excitation for each cell), which is dependent on the brightness of each cell.

The cells were excited using a fluorescence lamp with bandpass filtering. For the excitation of GCaMP3 and VSFP-butterfly1.2 (mCitrine excitation) we used a 480/40 $nm$ bandpass filter, for the excitation of R-GECO1 a 560/40 $nm$ bandpass filter was used. The fluorescence emission was collected for GCaMP3 at 535/40 $nm$ with the filter D535/40m (Chroma), for VSFP-butterfly1.2 (mKate, 594 $nm$) and R-GECO1 (624/40 $nm$) the filter HQ580/14m (Chroma) was used.

## 7.3 Data Analysis

Data from electrophysiological recordings were exported to Matlab (version 2011, Mathworks) and postanalyzed together with the fluorescence recordings which were already acquired in Matlab. For each cell at each trial, fluorescence images were recorded simultaneously to membrane voltage changes. Corresponding to the current-clamp protocols, sequences of fluorescence images were recorded. Furthermore, for each cell a region of interest (ROI) was manually selected per mouse click and a mean value was calculated by averaging the pixels from the selected ROI. Our program transformed each image series (for each trial) from the 3 dimensional space (X versus Y versus time) into the 2 dimensional space (mean fluorescence value versus time). Photobleaching was corrected using the *detrend* command in Matlab. The change in fluorescence was measured by the SNR [ Yamada and Mikoshiba, (2012) ].

It is calculated as the ratio of the *fluorescence signal* (F) and the standard deviation (SD) of *baseline fluorescence* (baseline), as seen in equation 7.1. With baseline fluorescence the fluorescence level immediately before the stimulus onset of the current clamp protocol is meant.

$$SNR = \frac{F - baseline}{baselineSD} \tag{7.1}$$

To quantify the efficiency of the proteins, the percentage of detected spikes compared to the total number of evoked spikes was calculated. Statistical difference between control and experiment was assessed using independent student's t-test. For the comparison between two groups a paired t-test or one-way ANOVA was used. A p-value of $< 0.05$ shows significant results.

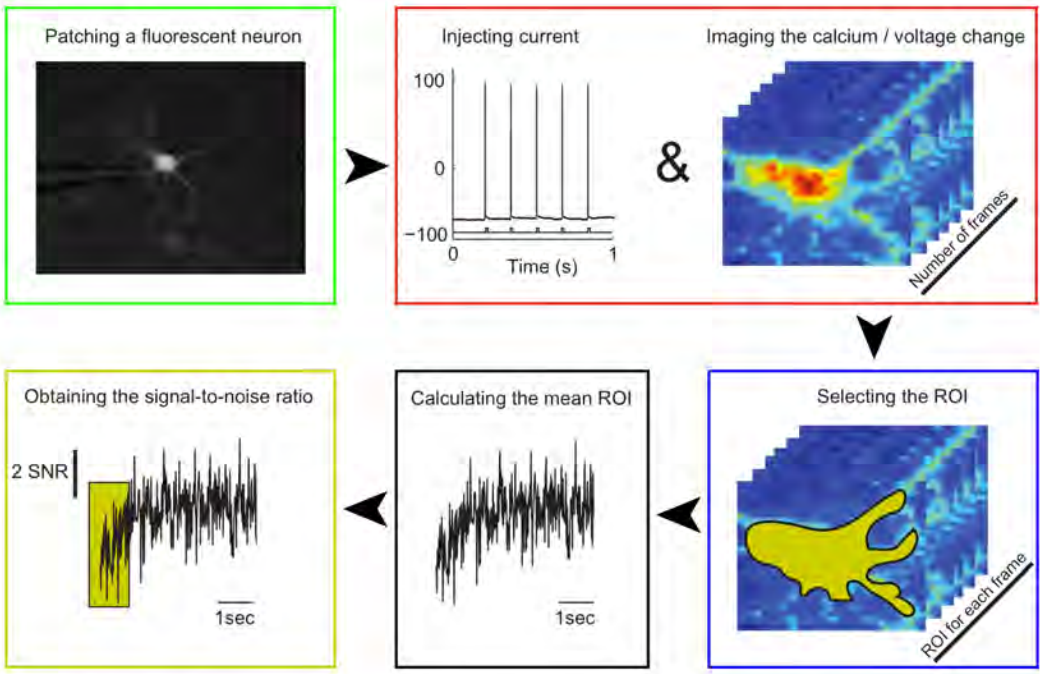


**Figure 7.1:** Methodological scheme of data acquisition and analysis. Hippocampal cultures were patched on the soma. Various current injections (square pulses with 10, 5, 3, 1.5 and 0.7 $Hz$, 1 $ms$ duration and 400 $pA$) were applied to the neurons at the same time as the data was imaged. Subsequently, a standard region of interest was selected and one mean value was calculated from all the pixels composing the chosen ROI for each of every recorded frames. The mean values of each frame were then plotted in sequence (corresponding to the x axis - time), and the SNR was measured.

CHAPTER 8

# Results

This chapter shows how selected genetically encoded indicators can be expressed in primary hippocampal neuron cultures. Furthermore, it presents how well membrane changes in cells can be detected by the emission of fluorescence. These membrane changes involve APs as well as synaptic inputs. Finally, we demonstrate that the fluorescence signal can also be used in order to detect synchronous activities. Supplementary elaborations can be found in [ Munguba, (2013) ].

## 8.1 Various GEIs Can be Expressed in Hippocampal Neuron Cultures

We transfected primary hippocampal neuron cultures with the genetically encoded indicators GCaMP3, R-GECO1 and VSFP-butterfly1.2 and investigated their expression 7-14 DIV after the transfection (see Fig. 8.1). As one can see, the VSFP-butterfly1.2-transfected cells showed expression of the fluorescent protein throughout the whole neuron, including the cell body, the axon and the dendrites. With the VSFP even dendritic spines and some intracellular structures were visible, allowing optical studies of activities in the whole neuron. On the other hand, also the GCaMP3- and R-GECO1-tranfected neurons showed good expression in the soma, axon and dendrites but with a more prominent absence of fluorescent protein expression in the nucleus. This could be an indication for the perfect synthesis of the two GECIs. [ Tian and Looger, (2008) ][ Yamada et al., (2011) ]

## 8.2 VSFP-expressing Neurons Revealed Lower Input Resistance

Since the goal of this study was to proof the potency of GCaMP3, R-GECO1 and VSFP-butterfly1.2 to monitor neuronal activities like APs and synaptic inputs by the expression of fluorescence, we performed electrophysiological experiments on each of the indicators. The criteria we used in order to ensure comparability within the indicators were the cells input resistances in $M\Omega$ and their resting membrane potentials in $mV$. We compared these values between

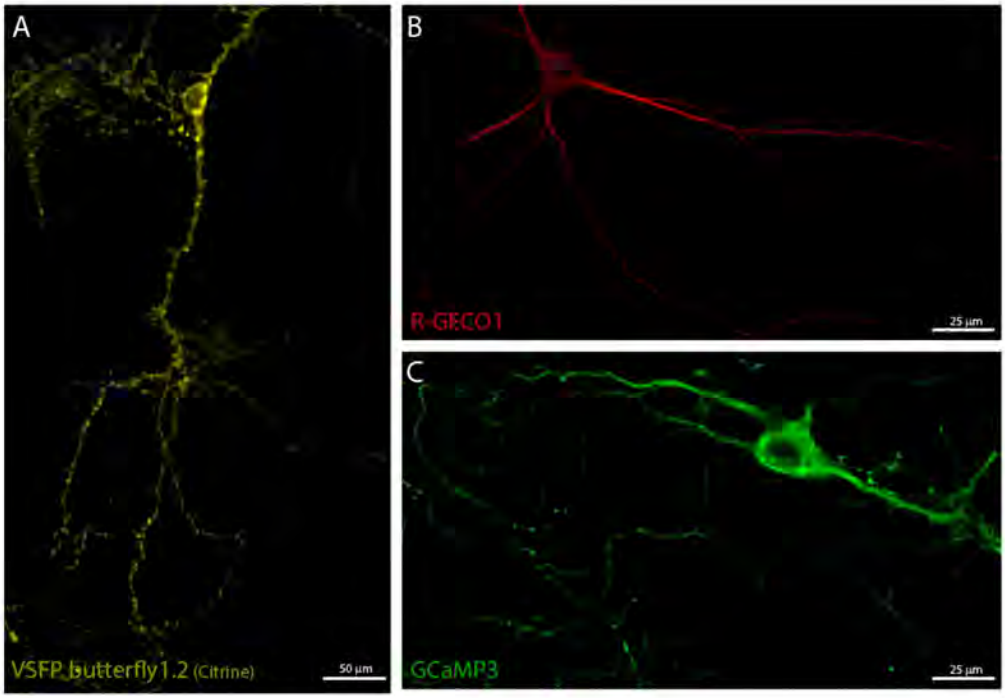


**Figure 8.1:** Genetically encoded indicators expressed in hippocampal neurons. A This figure shows the fluorescence image of a VSFP-butterfly1.2-expressing neuron (fluorescence for mCitrine). B: R-GECO1 is expressed in hippocampal neurons with no nuclear expression. C: The calcium indicator GCaMP3 is expressed throughout the whole neuron, except the nucleus.

the groups and detected that the VSFP-butterfly1.2-expressing neurons had a significant lower input resistance compared to GCaMP3-expressing neurons (p = 0.02), using one-way ANOVA followed by Tukey's range test. Following Ohm's law that $Voltage = Resistance * Current$ this would mean that the VSFP-butterfly1.2-expressing neurons need a higher current in order to reach the same voltage level as the other two neuron types. This could be an indication that the expression of VSFP alters a neuron's nature [ Mutoh et al., (2011) ], but interestingly the resting membrane potentials of the cells showed no significant differences between the three groups (p = 0.86), using one-way ANOVA (see Table 8.1).

| Parameter | GCaMP3 n=10 | R-GECO1 n=4 | VSFP n=15 | p-value |
|---|---|---|---|---|
| Input Resistance ($M\Omega$) | 161 $\pm$ 18.3 | 128 $\pm$ 15.3 | 94 $\pm$ 14.0 | 0.02 |
| Resting Membrane Potential ($mV$) | -56 $\pm$ 8.0 | -57 $\pm$ 2.5 | -60 $\pm$ 3.9 | 0.86 |

**Table 8.1:** Electrophysiological parameters

## 8.3 Calcium Indicators Have Higher SNR with Evoked APs

We performed whole-cell current clamp recordings, including current pulses with different frequencies (10, 5, 3, 1.5 and 0.7 Hz), and imaged the corresponding fluorescence emission of the patched neurons. [ Tian et al., (2009) ] were able to detect individual APs from GCaMP3 expressing neurons at 6 $Hz$. Our aim was to investigate if it is possible to detect APs with even higher frequencies and distinguish the individual spikes. In our experiments 80 % (n = 8 out of 10) of the GCaMP3-expressing neurons, 50 % (n = 2 out of 4) of the R-GECO1-expressing neurons and 26.7 % (n = 4 out of 15) of the VSFP-butterfly1.2-expressing neurons showed a detectable fluorescence signal in the soma in response to evoked APs. Only these expressing cells were further considered in this study.

The SNR of the soma for each group, when applying five current injections at 10 $Hz$ did not result in significant differences between the three GEIs (p = 0.25), using one-way ANOVA (see Table 8.2). Although the mean SNR for the VSFP-butterfly1.2 was the smallest, its fast kinetics allowed the detection of individual APs as clear distinguishable peaks in the captured fluorescence signal. For the calcium indicators the opposite was observed. In average they had a greater change of fluorescence but the kinetics seemed not as fast as the kinetics of the VSFP-butterfly1.2 when applying a pulsed 10 $Hz$ stimulus protocol and the discrimination of single APs from the fluorescence signal was more difficult.

Studies from [ Hires et al., (2008) ] investigated the $Ca^{2+}$ signal primarily in dendrites which motivated us also to look at the SNR values from dendritic projections. Therefore, we compared the two calcium indicators using an independent samples t-test. GCaMP3 and R-GECO1 showed similar SNR values (p = 0.52), both for the dendritic signal as well as for the somatic signal (see Table 8.2). Opposing the somatic SNR to the dendritic SNR, we found no significant differences, neither for GCaMP3 (p = 0.23), nor for R-GECO1 (p = 0.52).

| SNR | GCaMP3 n=8 | R-GECO1 n=2 | VSFP n=4 | p-value |
|---|---|---|---|---|
| Somatic | 21± 6.69 | 52 ± 19.70 | 13 ± 0.21 | 0.25 |
| Dendritic | 14 ± 4.0 | 18 ± 3.13 | - | 0.52 |

**Table 8.2:** Signal-to-noise ratio

## 8.4 The GEIs Have a Similar AP Detection Rate

In order to quantify how many of the evoked APs could be reported in the fluorescence emission, we aligned the optical recordings with the electrophysiology data and counted the peaks in the fluorescence emission. None of the indicators was able to detect all evoked APs when applying a pulsed 10 $Hz$ stimulus protocol. Among the GCaMP3-expressing neurons (n = 8), 54 % of the APs could be optically detected at the soma. From the R-GECO1 (n = 2) emission we were able to detect 85 % of the evoked APs and from the VSFP-butterfly1.2 (n = 4) signal 54 % could

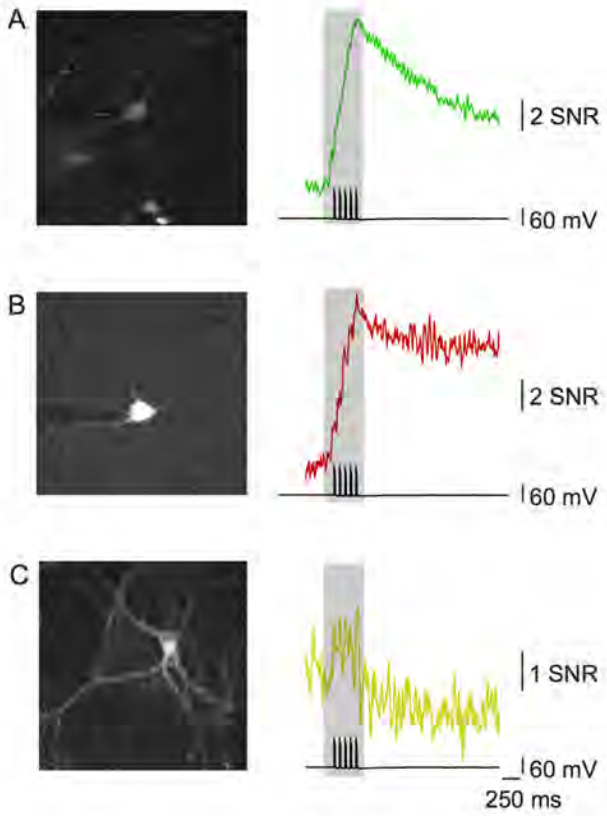


**Figure 8.2:** SNR of selected fluorescence signals from individual neurons. This figure shows a patched neuron (left) and its fluorescence response (right) caused by 5 APs due to a pulsed 10 $Hz$ stimulation. A: This GCaMP3-expressing neuron reached a SNR of almost 20 in its calcium response. B: Although the soma was very bright, the SNR of this R-GECO1-expressing neuron was quite low. C: The SNR of the fluorescence signal of this VSFP-butterfly1.2-expressing neuron after removing the linear trend and emphazising the peaks is shown.

be detected. One-way ANOVA showed no significant differences between the AP detection rate of the three GEIs when considering the fluorescence signal at the soma ($p = 0.26$). Selected examples of somatic and dendritic SNR are shown in Fig. 8.2.

While both GECIs allowed the detection of single APs also when varying their frequencies (see Fig. 8.3), the problem of detecting spikes from the VSFP-butterfly1.2 signal was the relatively high background noise in the fluorescence signal. This noise made the distinction between evoked APs and ongoing background activities quite difficult. Only with the alignment to the electrophysiological data we were certainly able to detect the spikes. Also subthreshold signals could not be reported robust enough in order to disregard the patch clamp recordings.

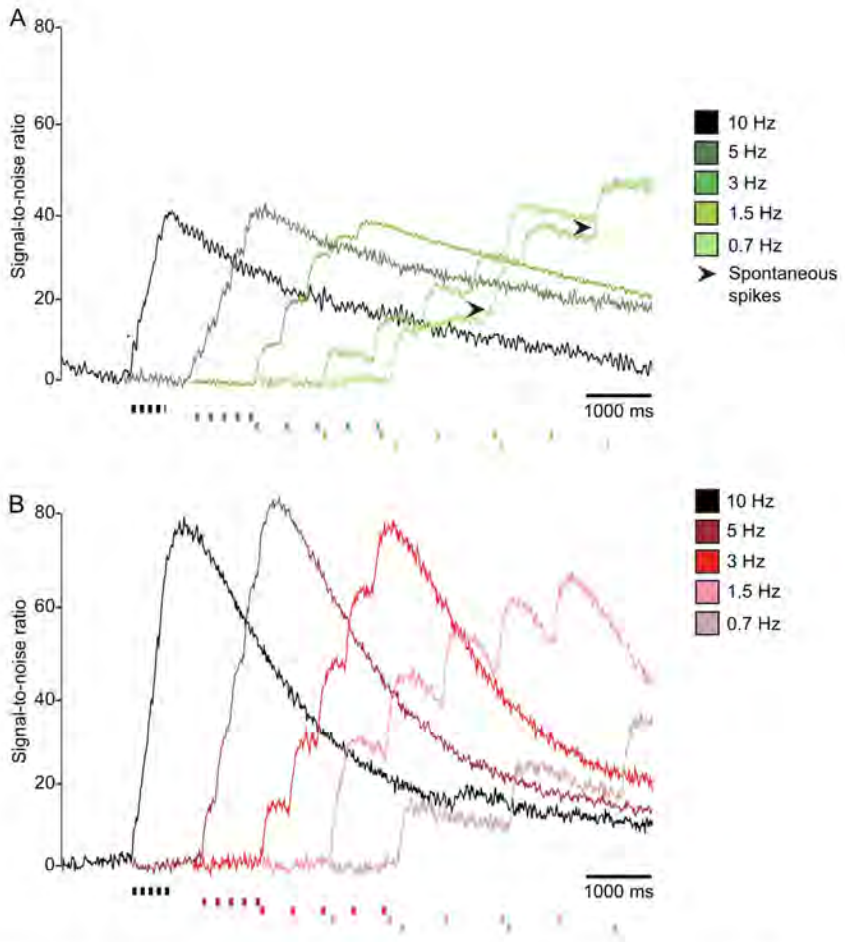


**Figure 8.3:** Calcium imaging with different action potential frequencies. This figure shows the SNR values of the two calcium indicators GCaMP3 (A) and R-GECO1 (B) in response to five evoked APs with 10, 5, 3, 1.5 and 0.7 $Hz$. Single APs could be clearly detectable from the fluorescence signal throughout the different frequencies. Arrow heads in A indicate spontaneous spikes detected with the current-clamp recordings.

Since the somatic detection of APs worked quite well for GCaMP3 and R-GECO1, we also compared the dendritic fluorescence emission. With the fluorescence signal of GCaMP3 (n = 6, 2 neurons did not show enough dendritic fluorescence emission) we were able to detect 62.2 % of the evoked APs. The signal for R-GECO1 (n = 2) even led to 100 % AP detection. But due to the low number of probes, we could not certainly conclude that the spike detection on dendrites worked sufficiently. An independent samples t-test showed no significant difference between the two GECIs (p = 0.14).

## 8.5 GECIs are able to Report Spatial Differences

Besides the temporal analysis of the fluorescence signals, we also analyzed the possibility of GEIs to monitor spatial activities. Due to the higher SNR of GCaMP3 and R-GECO1 compared to the VSFP-butterfly1.2, we show only results of the GECIs in the following sections.

With the calcium indicator GCaMP3 we were able to distinguish the origin of both action potentials and synaptic potentials at different parts of the neuron. Fig. 8.4 A shows four neurons, one of them patched and stimulated with a pulsed current injection at 10 $Hz$. The obtained fluorescence signal showed a good temporal, but more importantly, also a very good spatial resolution. Only the stimulated neuron caused a change in the fluorescence signal, the others stayed the same (see Fig. 8.4 B).

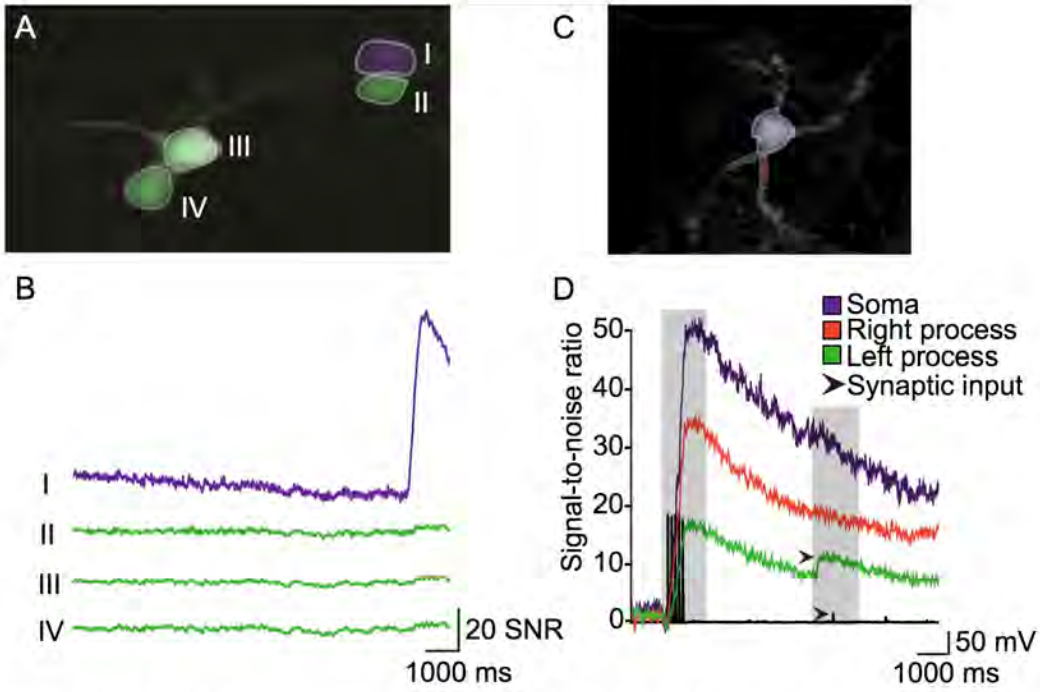


**Figure 8.4:** Spatial discrimination with GCaMP3. This figure shows that there are spatial differences in SNR of GCaMP3, according to the occurrance of membrane activity changes. A: Simultaneous imaging of four GCaMP3-expressing neurons. B: GCaMP3 allowed the discrimination of activated and silent cells with high spatial and temporal resolution. C: Patched neuron expressing GCaMP3 with ROI for the soma (purple) and ROI for two different processes (green and red). D: Current clamp recordings (5 evoked APs with 10 $Hz$) and SNR values from three different parts of the same neuron (see C) identified the origin of a synaptic potential (arrow heads).

Looking at only one cell, but different selected parts of the neuron, we observed that there was also a notable difference in the fluorescence emission, indicating the spatial difference of the action potential movement. Moreover, we were able to detect the origin of an excitatory post-synaptic potential in the fluorescence signal. The current-clamp recordings from the soma of the neuron showed this subthreshold membrane depolarization, which could also be seen in the SNR of the different parts of the neuron (see Fig. 8.4 C and D). Similar observations could also be seen with the calcium indicator R-GECO1.

While evoked APs are mainly triggered by the opening of voltage-sensitive $Ca^{2+}$ channels, as a consequence to the injected, depolarizing currents, synaptic potentials originate from various membrane mechanisms, such as the opening and closing of N-methyl-D-aspartate (NMDA) receptors, 2-amino-3-(3-hydroxy-5-methyl-isoxazol-4-yl)propanoic acid (AMPA) receptors and also voltage-sensitive $Ca^{2+}$ channels [ Müller and Connor, (1991) ][ Higley and Sabatini, (2008) ].

## 8.6 Somatic Calcium Signals from APs and Synaptic Potentials Are Similar

In Fig. 8.4 D we show that it was possible to detect synaptic potentials in the fluorescence signal of calcium indicators. Interestingly, the synaptic input could be observed very well in the dendrite. In the soma however it could not be seen that clearly. Therefore, we investigated the fluorescence signal due to synaptic potentials more detailed on the soma, the dendrite and a dendritic spine, which typically receives the input of a presynaptic neuron through a single synapse. We further compared these three signals with the fluorescence changes at the same locations but caused by evoked APs at the soma.

Fig. 8.5 shows a neuron, with a spontaneously occurring synaptic potential. This potential caused a membrane voltage change of approximately 30 $mV$. The same neuron was also stimulated with a pulsed 10 $Hz$ current injection. Interestingly, the somatic SNR values of these two different neuronal activities were nearly the same (the values were approximately 70).

Although evoked APs and synaptic potentials have a different origin and also distinct biophysical meanings, they had a very similar SNR. Comparing the dendritic fluorescence emission, the synaptic potential yielded to a SNR of about 110, whereas the evoked APs reached only a SNR of 35. Even more interestingly is the signal at the dendritic spine. When evoking APs at the soma, no signal at the dendritic spine could be reported, but during the synaptic potential a SNR of approximately 30 could be registered.

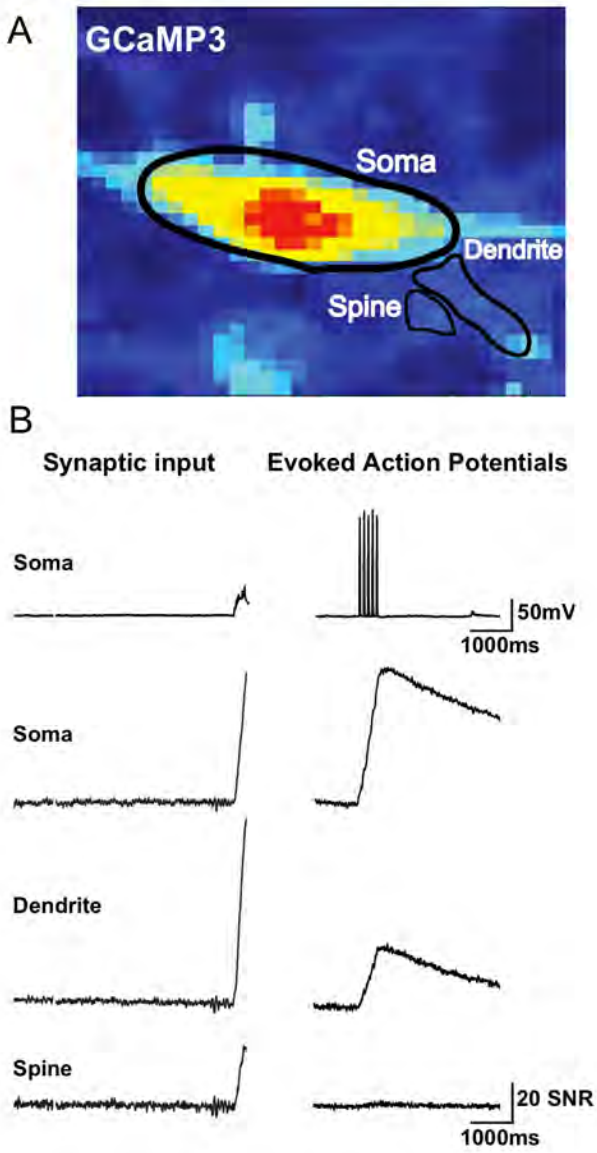


**Figure 8.5:** Evoked APs versus synaptic inputs. A: This figure shows a patched GCaMP3-expressing neuron with three different fluorescent parts: soma, dendrite and spine. B: Spontaneous synaptic potentials led to a ~30 $mV$ membrane potential change resulting in a SNR of ~70 at the soma, ~110 at the dendrite and ~30 at the spine (left). Imaging of 5 evoked APs caused smaller SNR values: The values were ~70 at the soma (comparable to the synaptic potential), ~35 at the dendrite and no detectable fluorescence change at the spine (right).

## 8.7 Calcium Indicators Can Detect Spontaneous APs

Since there was no notable difference between the somatic SNR of a spontaneous potential and the somatic SNR or an evoked potential with GCaMP3, we investigated if the R-GECO1 signal was able to distinguish between evoked action potentials at the soma and spontaneous appearing APs. Surprisingly, patch clamp recordings showed that spontaneous APs had a lower SNR than evoked APs in R-GECO1-expressing neurons (Fig. 8.6). The evoked APs caused a SNR of approximately 90, whereas the spontaneous AP only reached a SNR of around 25. Comparing the somatic signal with the calcium signal from one process of the neuron, we saw that there was no fluorescence change happening in this process. We believe that this particular recording represents a situation where the synaptic potentials arrived directly at the soma.

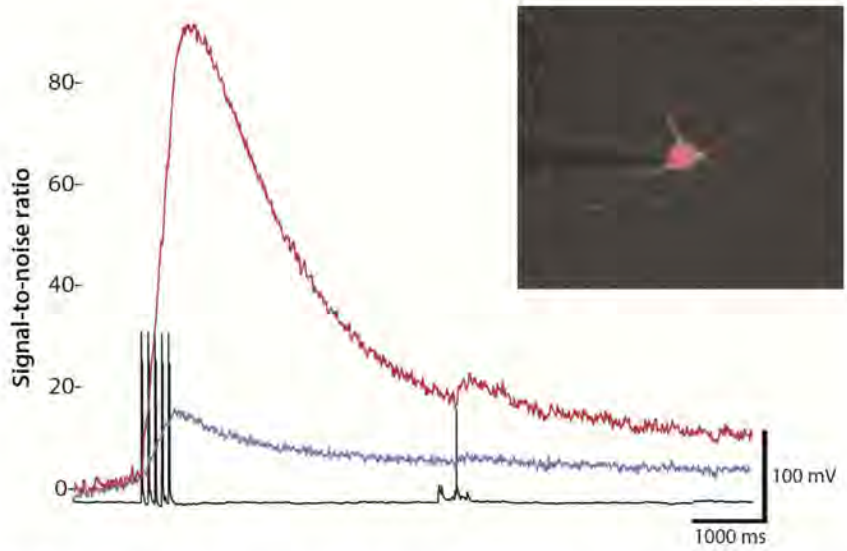


**Figure 8.6:** Detection of spontaneous APs from a R-GECO1-expressing neuron. Current clamp recordings of an R-GECO1-expressing neuron showed a spontaneous AP that could be detected with calcium imaging at the soma (red). But no calcium signal was detected at the investigated process (blue).

## 8.8 GCaMP3 Reports Neuronal Network Synchronization

The difference in calcium signals resulting from APs and synaptic potentials motivated us to use calcium imaging for the study of neuronal network connectivity and synaptic signal transfer. Indeed, during our experiments we saw that possible neuronal network synchronization could be detected by the use of GECIs. Imaging groups of cells, we were able to distinguish active from silent neurons with the GCaMP3 signals. Moreover, we were able to monitor synchronized activity, as shown in Fig. 8.7.

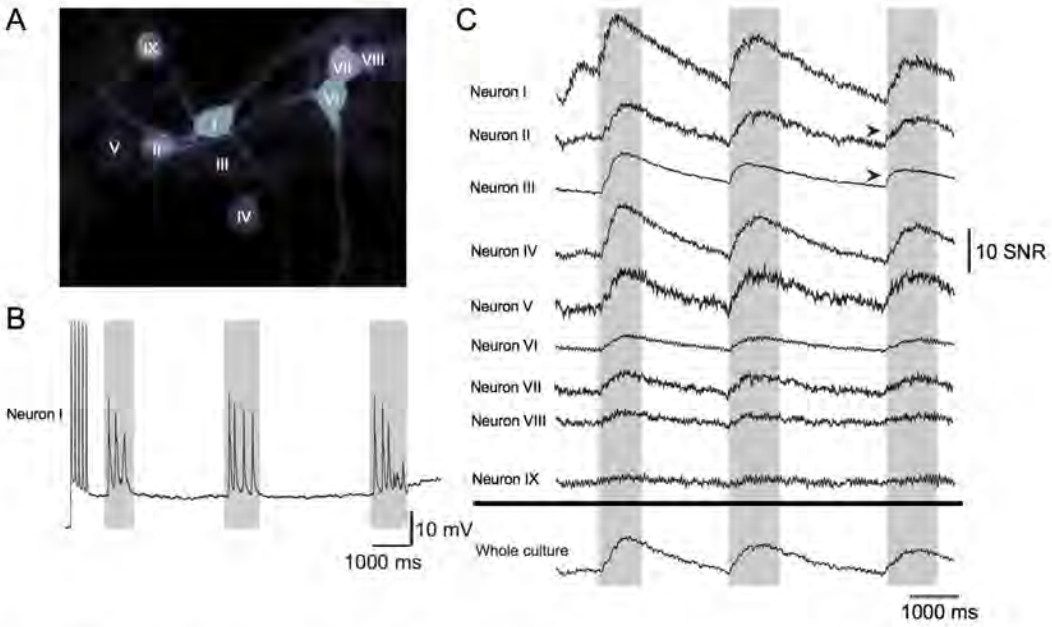


**Figure 8.7:** Synchronous activity of a neuron group. A: This figure shows a fluorescence image of nine GCaMP3-expressing neurons. B: Neuron I was patched and five APs were evoked by a pulsed current injection (10 $Hz$). This cell also showed three spontaneous potentials afterwards. C: With calcium imaging we were able to detect that eight other neurons were also activated, with their responses after the spike train in neuron I. Arrow heads indicate that neuron II and III were active before neuron I received the synaptic inputs, suggesting that these two neurons led to the synaptic potentials seen with the soma recordings and the calcium signal from neuron I.

One cell (neuron I) was stimulated with a pulsed 10 $Hz$ current injection causing the generation of APs. Furthermore, it received synaptic inputs from other neurons, which can be clearly seen in the electrophysiology data by the spikelets in the voltage trace. Analyzing the fluorescence signal of the surrounding cells, we saw that seven other neurons were activated by the evoked APs of neuron I. The fluorescence changes of the seven other neurons occurred chronologically after the APs happened in neuron I. As one can see, not all of the captured cells showed neuronal activity. Neuron IX for example remained silent, suggesting that GCaMP3 is a reliable indicator in order to distinguish between active and silent neurons.

Moreover, from the sum of the fluorescence changes of the eight active cells, one could see that a synchronous activity occurred, indicated by the synchronized SNR changes of the cells. We also saw that the neurons II and III spiked slightly before neuron I, which could be an indication that these two neurons initiated the postsynaptic potentials seen in neuron I, in both the fluorescence signal as well as the electrophysiological recording.

## 8.9 Carbachol Causes Synchronized Activities in Hippocampal Neuron Cultures

Carbachol was shown to induce synchronization in various in vitro and in vivo studies [ Bianchi and Wong, (1994) ]. When applying carbachol (10 $\mu M$, bath-applied) to our cultures, we could also observe the formation of synchronized activities between the cells (see Fig. 8.8). The SNR of the single neurons as well as the SNR of the whole culture suggest a dependent, synchronized activity throughout the whole culture. These SNR values were much higher than in cultures without carbachol applied, possibly resulting from the higher calcium influx through the carbachol-activated acetylcholine receptors.

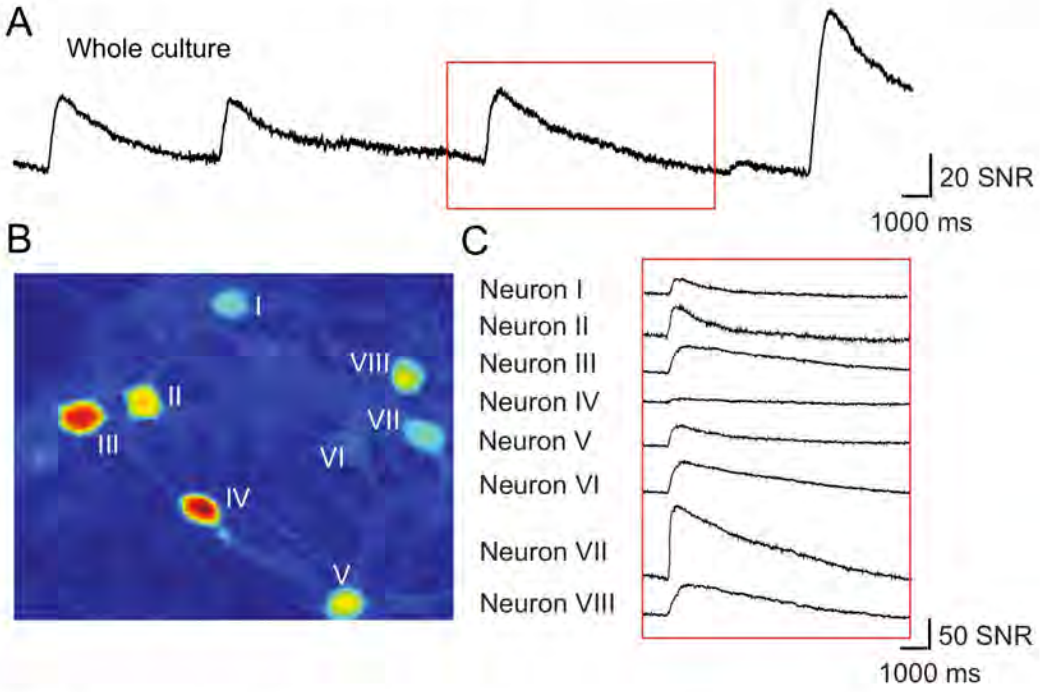


**Figure 8.8:** Carbachol-induced synchronous activity of cultured neurons. A: This figure shows that carbachol (10 $\mu$) led to synchronized activities in hippocampal neuron cultures (considering all cells together) B: With the GCaMP3-expressing neurons we were able to detect these coherent activities. C: Calcium imaging of eight individual cells demonstrated synchronous SNR value changes.

CHAPTER 9

# Discussion

Since a few years, optogenetics has become more and more present in brain research, and today it is already one of the most popular techniques in experimental neuroscience. Optogenetics is a combination of techniques from optics and genetics in order to activate and control neurons by light. Also the monitoring of neuronal activities can be done by light, usually fluorescent light. Therefore, reporter proteins have been engineered during the last few years. These reporter proteins are fluorescent proteins which change their fluorescence emission as a consequence of environmental changes, such as calcium concentration or voltage changes.

The present study includes a revolutionary approach of detecting neuronal activities by light. Therefore, the latest genetically encoded calcium indicators GCaMP3 and R-GECO1 and the genetically encoded voltage indicator VSFP-butterfly1.2 were introduced into primary hippocampal neuron cultures and their fluorescence emission was collected. We implemented a technique to express the three genetically encoded indicators in cultured neurons and captured the fluorescence response caused by transmembrane potential changes. Furthermore, we evaluated the reliability of this minimal invasive approach in order to detect action potentials. Up to date, GCaMP3, R-GECO1 and VSFP-butterfly1.2 are the latest genetically encoded indicators available and no other study has compared their potency in detecting APs yet.

Our findings were: (1) VSFP-expressing neurons revealed lower input resistances compared to GCaMP3- and R-GECO1-expressing neurons, suggesting a little variation in the physiology of the neurons; (2) GCaMP3-expressing neurons had the highest SNR with evoked APs; (3) all GEIs had a similar AP detection rate, but for the VSFP-signal the alignment with the electrophysiological data was necessary due to the high background noise; (4) AP firing with lower frequencies (up to 5 $Hz$) could be detected more certainly with GECIs than with GEVIs; (5) GECIs exhibited a high spatial resolution when detecting individual and multiple neurons simultaneously; (6) GECIs also could report synaptic potentials and spontaneous APs, but with varying calcium signals; (7) GCaMP3 was able to detect neuronal network synchronization.

## Considerations Using Optical Methods

When performing fluorescence experiments, an optimal optical setup is needed. This optimization concerns the use of fast cameras (with a large number of frames per second), specific filters according to the used fluorescent proteins, and highly magnifying objectives with large numerical apertures to minimize bleaching and virtually detect every photon reaching the sensor. Furthermore, analytical techniques become more and more important, both for a clear spike detection and the reconstruction of AP rates [ Yaksi and Friedrich, (2006) ] [ Vogelstein et al., (2009) ] as well as the experimental design itself. Although optogenetics gives us the great possibility of investigating almost every part of the brain we like, from whole brain regions to the level of single cells, well considered controls are necessary.

These controls involve expression studies, as well as functional studies. Therefore, we introduced our three genetically encoded indicators to HEK 293 cells first. These cells are relatively easy to work with and allow a pleasant transfection with various fluorescent proteins. Furthermore, they gave us the great possibility of investigating possible fundamental changes of electrophysiological properties due to the transfection. This means, we not only verified the fluorescence expression of the three GEIs in HEK 293 cell cultures, but also tested if any notable electrophysiological variations occurred. Therefore, we injected artificial (simulated) ionic currents to the cells, mimicking the activities of neurons. We could also define our stimulus protocols and camera settings based on these cells and compared our fluorescence signals with the literature. They confirmed with the SNR values obtained by [ Akemann et al., (2012) ].

## Various Criteria for GEIs

Nowadays, there are various genetically encoded indicators available, characterized by their dynamic range, different kinetics as well as the different light spectra they cover. Each of them has its own advantages and disadvantages.

GCaMP3, was chosen for this study because of its brighter fluorescence signal and its higher protein stability compared to its previous versions. Furthermore, GCaMP3 is the most extensively employed GECI, including the genetic targeting of specific subpopulations or subcellular compartments by using the Cre/lox system [ Tian et al., (2009) ][ Yamada et al., (2011) ][ Zhao et al., (2011) ][ Yamada and Mikoshiba, (2012) ].

R-GECO1 is a far-red-shifted fluorescent protein, and it was shown that it undergoes less significant phototoxicity due to its lower energy [ Dixit and Cyr, (2003) ]. Furthermore, a red-shifted FP has a longer wavelength range and therefore deeper tissue penetration, meaning that the light can reach deeper brain areas compared to blue-shifted FPs which can be of significance when performing in vivo experiments [ Zhang et al., (2008) ]. Also autofluorescence and absorption of light by tissues are decreased in the red-shifted probes [ Kremers et al., (2011) ]. The reduction of photodamage is due to the substitution of the GFP in GCaMP3 by the FP mApple. Its emission spectrum makes it very attractive to use in combination with other FPs, since no spectral overlaps are expected [ Shcherbo et al., (2009) ].

Voltage-sensitive fluorescent proteins on the other hand, were shown to have faster kinetics than calcium indicators which makes them more prone for the detection of APs. Although there exists a big variety of VSFPs covering different light spectra, the decision of using the VSFP-butterfly1.2 in this study is based on the good membrane targeting as well as the reported AP detection in vivo [ Akemann et al., (2012) ]). Furthermore, it consists of the far-red shifted protein mKate2, which brings the advantages of R-GECO1, less photodamage and higher tissue penetration.

### Side Effects of Using GEIs

Although the use of genetically encoded indicators represents a minimal invasive method, there are some considerations to make. Especially, when dealing with calcium indicators, one has to consider probable changes in the calcium buffering and other protein specific interactions due to variations in the calcium concentration. This can yield to the alteration of a neuron's action potentials, especially their amplitude and duration.

In our study both GCaMP3 and R-GECO1 were expressed throughout the whole cell, reaching the full size of the neurons (see Fig. 8.1). There was no nuclear labeling observed. The expression was limited only to the cytoplasm. This is an indication for the healthiness of the neuron and an ideal synthesis of the indicator. Other studies using GCaMP3 showed that the expression in some cases can include the nucleus of the neurons, but can cause impaired calcium homeostasis and function of GCaMP3 [ Tian et al., (2009) ]. Thus, we aimed to only choose neurons with expression in the cell's cytoplasm rather than its nucleus. When including neurons with protein expression in the nucleus (such as neuron III and IV in Fig. 8.8), we observed that they responded similarly to the other neurons, which had expression only in the cytoplasm. No electrophysiological or structural changes could be detected.

These possible alterations in neuronal activities remain discussable. Studies expressing GCaMP2 in cortical cells, the previous version of GCaMP3, showed attenuated responses due to APs in neurons [ Hires et al., (2008) ]. Contradictory, other studies also using GCaMP2 in cortical neurons did not observe any connection to the healthiness of the cells [ Mao et al., (2008) ].

However, not only calcium indicators can cause possible cell alterations. Also the expression of voltage indicators can yield to perturbations in neurons. Our experiments showed a lower input resistance for VSFP-expressing cells (see Table 8.1), which might be an indication that its expression affected the neuron [ Mutoh et al., (2011) ]. This lower input resistance might also suggest some stage of immaturity [ Fukuda et al., (2003) ], although our patched cells showed normal electrophysiological responses to evoked APs. The input resistance displays the cell size and can give information about the membrane channels opened when the cell is at rest. A lower resistance usually implies a higher density of open channels, which can be a possible explanation since the introduction of a genetically introduced protein such as the VSFP-butterfly1.2 forces the rearrangement of the cell's membrane, yielding to a possibly different cell synthesis.

### Action Potential Detection

Although the various transfected neurons had resting membrane potential values as expected (see Table 8.1), not all of them were able to report action potentials by their fluorescence signals. While 80 % of the GCaMP3-expressing neurons (n = 8 out of 10) exhibited a detectable fluorescent emission, only 50 % of the R-GECO1-expressing cells (n = 2 out of 4) and 26.7 % of the VSFP-butterfly1.2-expressing cells (n= 4 out of 15) provided a detectable fluorescence signal (see Table 8.2). Due to the low number of experiments with R-GECO1 there was no certain statement about the AP detection rate possible. However, our GCaMP3 investigations seem promising and suggest a good AP detection power of this type of calcium indicator. Although this is contradictory to studies from [ Mao et al., (2008) ] and [ Tian et al., (2009) ], we believe that until now GCaMP3 has a higher reliability of reporting APs than voltage indicators. Also [ Akerboom et al., (2012) ] could show that GCaMP5, which is the newest version of GCaMP, is able to detect single spikes in vitro. This is quite promising since calcium indicators seem to have a higher SNR compared to voltage indicators.

Also our experiments for the VSFP-butterfly1.2-expressing neurons showed a quite low SNR compared to the GCaMP3- and R-GECO1-expressing neurons (see Table 8.2). Studies from [ Knöpfel et al., (2010) ], [ Akemann et al., (2010) ] and [ Akemann et al., (2012) ] reported a relatively low SNR for voltage indicators as well. Our experiments confirm with their SNR values. Nevertheless, it was unexpected that only one fourth of the cells showed a detectable SNR due to evoked APs (see Fig. 8.2).

One reason for this big difference in SNR of the used voltage indicator compared to the two calcium indicators could be the fact that VSFP-butterfly1.2 uses a FRET-based pair of fluorescent proteins which can cause this low SNR. As shown in chapter 4 the efficiency of FRET is inversely proportional to the sixth power of the distance between the two fluorescent proteins, which makes the energy transfer from the donor to the acceptor fluorophore very sensitive and difficult to find out if the low expression is a result of the FRET mechanism [ Harris, (2010) ]. One could capture the emission of the excited FP directly, instead of collecting the fluorescence signal from the second FP in order to measure the level of expression without FRET and detect possible weaknesses in the energy transfer [ Miyakawi and Tsien, (2000) ].

One of the strengths of voltage-sensitive fluorescent proteins though, are the fast kinetics, which are able to separate individual APs even at high frequencies. Thus, also VSFPs seem very promising, but still have to be improved in order to detect single APs. In our experiments we could not disregard the electrophysiological recordings of the VSFP-butterfly1.2-expressing neurons for a reliable AP detection in time. But how reliable is the AP detection with standard electrophysiological methods anyways?

### Artifact-free Recordings

Classical electrophysiological approaches suffer from different environmental artifacts and need complicated, sometimes unreliable, methods [ Rattay, (1999) ]. In top of that, extracellular stimulation techniques usually do not excite synapses, as biophysiologically realistic, but evoke action potentials at the soma [ Rattay, (1999) ]. Thereby, locally, very high potentials are needed, much higher than the 20 $mV$ needed to depolarize the membrane above the AP threshold. Also current injections at a single point (where the cell is patched) are usually very high, due to the small pipette tip. The smaller the area (pipette diameter), the higher is the current density at that point, meaning that more current is flowing in a defined space if the area is smaller. Depending on the AP initiation site this can result in very arbitrary phenomena [ Rattay et al., (2012) ]. [ Rattay and Wenger, (2010) ] investigated various mechanisms of extracellular stimulation and discussed the difficulties one has to deal with when using invasive approaches. [ Brown et al., (1996) ] for example used a masking function in order to measure artifact-free neuronal responses.

However, the recent developments of optogenetical methods provide new possibilities for functional studies of neurons, with several advantages over purely electrophysiological methods. Since optical recordings are relatively non-invasive, they do not suffer from artifacts as much as electrical methods do. If the neuron expresses a fluorescent reporter and is spontaneously active, meaning that it generates APs by its own, no microelectrode needs to be inserted in order to study its spiking properties. The optical setup is passive and does not need to actively influence the neuron. Even if fluorescent neurons need to be excited by light in order to measure evoked signals, optical approaches already offer various techniques preventing photobleaching or phototoxicity, e.g. the aforementioned far-red shifted proteins, which seem to be less harmful than an extracellular stimulation with a micropipette.

Furthermore, using optical approaches allows us to capture spatially different regions and study their dynamics. Especially, when capturing a group of synchronizing cells, both temporal and spatial properties should be taken into account. Therefore, optical methods seem to be very convenient.

### Spatial Resolution

Since long it is believed that neurons spike according to the *all-or-none principle*, meaning that they will either generate an AP or not, there is no "half" action potential. When a neuron receives excitatory inputs, its sodium channels open and allow $Na^+$ to flow into the cell. This causes the depolarization of the cell and, if a certain threshold is reached, the generation of an AP. In order to reach the AP threshold, the neuron needs to get sufficiently depolarized. Neurons receive millions of synaptic inputs from other neurons, which contribute differently to the depolarization of the neuron. Some inputs are received very distal, some more proximal (close) to the soma and depending on the intensity or summation of these inputs, they can either disperse or trigger an AP. [ Hille, (1992) ]

Pure electrophysiological techniques usually allow the observation of electrical activities only at a single point within the investigated tissue. This means, standard electrophysiological techniques normally cover more the local, single activities of neurons than the distributed phenomena. But exactly this spatial distribution of tasks is what makes our brains so powerful compared to all other systems. Optical methods have the great possibility of capturing the spatial expansion of neuronal activities, especially in combination with molecules emitting fluorescent light in response to chemical and electrical environment changes.

As seen in Fig. 8.4) and 8.7, we were able to monitor spatially separated inputs with genetically encoded calcium indicators. We were able to distinguish between active and silent neurons, as well as evoked APs and synaptic inputs at different parts of the neuron. Furthermore, we could use the expression of the GCaMP3-expressing neurons to monitor ongoing neuronal synchronization (see Fig. 8.7 and Fig. 8.8).

When analyzing the SNR values collected from the soma and dendrites (see Fig. 8.5), in order to detect synaptic inputs, we saw that the dendritic SNR was higher than the somatic SNR for synaptic inputs, but the opposite was the case (the dendritic SNR was lower than the somatic SNR) for evoked APs. While the dominant source of calcium influx due to evoked APs through voltage-sensitive calcium channels is found in the plasma membrane [ Jaffe et al., (1992) ], calcium influx coming from synaptic inputs has different sources, such as NMDA receptors, subtypes of AMPA receptors, internal storages, as well as voltage-sensitive calcium channels [ Higley and Sabatini, (2008) ]. However, since it is believed that the soma is the part where the summation of the synaptic inputs takes place, dendritic signals are less representative to express a neuron's activity.

Also when comparing evoked APs with spontaneous occurring ones as in Fig. 8.6, we saw that spontaneous APs caused only a change in the somatic fluorescence emission, whereas the evoked one caused a change in both, the somatic as well as the dendritic fluorescence emission. Another argument for using the somatic rather than the dedritic SNR is the problem when recording from larger populations or thicker brain slices, where a reduced spatial resolution is available because of the compact nature of the dendrites. [ Arieli et al., (1995) ]

## Conclusion

Our evaluation of the three genetically encoded indicators GCaMP3, R-GECO1 and VSFP-butterfly1.2 allows a better understanding on many sides of the application of such proteins in order to study neuronal activities in a minimal invasive way.

Although we encountered indicatives that physiological disturbances are possible to occur in expressing neurons, such as seen within the neurons expressing VSFP-butterfly1.2, we demonstrated that genetically encoded reporters are a considerable alternative to electrophysiological methods. The application of the VSFP-butterfly1.2 in this study still required the benefits from classical electrophysiological approaches in order to report neuronal events with high temporal resolution, but VSFPs represent a reasonable option for monitoring neuronal activities.

Our results also suggest that the available calcium indicators allow detailed studies of neuronal activities, especially when investigating sparse spiking neurons. This ranges from individual dendritic spines to the investigation of synchronizing events in neuronal networks. But compared to voltage indicators, calcium indicators have slower kinetics.

Nevertheless, reliable standardizations and consistent controls must be primarily established in order to employ such optogenetical tools in a trustworthy manner.

APPENDIX A

# Abbreviations

**ANEP** aminonaphthylethenylpyridinium

**AP** action potential

**CaM** calmodulin

**CCD** charge-coupled device

**cDNA** complementary deoxyribonucleic acid

**CFP** cyanfluorescent protein

**CMOS** complementary metal-oxide-semiconductors

**CMV** cytomegalovirus

**cpFP** circularly permuted fluorescent protein

**DAPI** 4' 6-diamidino-2-phenylindole

**DIC** Differential interference contrast

**DIV** day in vitro

**DMEM** Dulbecco's modified eagle medium

**DNA** deoxyribonucleic acid

**E. coli** Escherichia coli

**EGFP** enhanced green fluorescent protein

**EMEM** Eagle's Minimum Essential Medium

**FBS** fetal bovine serum

**FP** fluorescent protein

**FRET** fluorescent resonance energy transfer

**GEI** genetically encoded indicator

**GECI** genetically encoded calcium indicator

**GEVI** genetically encoded voltage indicator

**GFP** green fluorescent protein

**HEK** human embryonic kidney

**LED** Light-emitting diode

**LFP** local field potential

**mRNA** messenger ribonucleic acid

**Osm** osmolars

**PBS** phosphate buffer saline

**PEST** penicillin streptomycin

**R-GECO1** red-genetically encoded $Ca^{2+}$. optical indicator 1

**ROI** region of interest

**RTAI** Real Time Application Interface

**standard deviation** SD

**SNR** signal-to-noise ratio

**VSD** voltage-sensitive dye

**VSFP** voltage-sensitive fluorescence protein

**VSFP** yellow fluorescent protein

# APPENDIX B

# Source Code

**Listing B.1:** Host Code: ionic_currents.m

```
1  % Markus Michael Hilscher – 0727932
2  % Basket.m
3  % Model of a fast–spiking interneuron
4
5  clear;
6  tic
7
8  %% User Input
9  EndOfSimulation = 700; % Simulation time in ms
10 dt = 0.05; % step for Euler
11 k = 5; % Wang and Buszaki (1996) show k = 5, 3.33 and 2
12                          % smaller phi –> IK is slower, AHP amplitude more negative
13 Stimulus = 0.25; % Wang and Buszaki (1996) show Stimulus = 1, 1.2 and 1.4 uA/cm^2
14 Starttime = 100; % starting time of the stimulus in ms
15 Endtime = 600; % ending time of the stimulus in ms
16 V = −64; % membrane voltage at the beginning in mV
17 Isyn = 0; % synaptic current in uA/cm^2
18
19 %% Constants
20 VNa = 55; % reversal potential of the Na+ current in mV
21 VK = −90; % reversal potential of the K+ current in mV
22 VL = −65; % reversal potential of the leak current in mV
23
24 gNa = 35; % conductance of the Na+ current in mS/cm^2
25 gK = 9; % conductance of the K+ current in mS/cm^2
26 gL = 0.1; % conductance of the leak current in mS/cm^2
```

```
27
28  Cmem = 1; % membrane capacitance density in uF/cm^2
29
30  xh = 0; % inactivation variable h
31  xn = 0; % activation variable n
32
33  t_rec = 0;
34  x_plot = zeros(1,EndOfSimulation/dt+1);
35  y_plot = zeros(1,EndOfSimulation/dt+1);
36  y_plot_Iion = zeros(1,EndOfSimulation/dt+1);
37  y_plot_INa = zeros(1,EndOfSimulation/dt+1);
38  y_plot_IK = zeros(1,EndOfSimulation/dt+1);
39  y_plot_IL = zeros(1,EndOfSimulation/dt+1);
40
41  %% Program
42  for t=0:dt:EndOfSimulation
43
44      if t>=Starttime;
45          Iapp = Stimulus;
46      else
47          Iapp = 0;
48      end
49      if t>Endtime;
50          Iapp = 0;
51      end
52
53      alpham = -0.1*(V+35)/(exp(-0.1*(V+35))-1); % alpha m
54      alphah = 0.07*exp(-(V+58)/20); % alpha h
55      alphan = -0.01*(V+34)/(exp(-0.1*(V+34))-1); % alpha n
56
57      betam = 4*exp(-(V+60)/18); % beta m
58      betah = 1/(exp(-0.1*(V+28))+1); % beta h
59      betan = 0.125*exp(-(V+44)/80); % beta n
60
61      taum = 1/(alpham+betam); % taum
62      x_0m = alpham*taum; % minf
63
64      xh = xh + dt* k*(alphah*(1-xh) - betah*xh); % dh/dt
65      xn = xn + dt* k*(alphan*(1-xn) - betan*xn); % dn/dt
66
67      INa = gNa*x_0m^3*xh*(V-VNa); % Na+ current
68      IK = gK*xn^4*(V-VK); % K+ current
69      IL = gL*(V-VL); % leak current
```

```
70
71      Iion = INa + IK + IL; % ionic current
72
73      V = V + dt*(-Iion -Isyn + Iapp) / Cmem; % membrane voltage
74
75      Vpre = V;
76
77      t_rec = t_rec+1;
78      x_plot(t_rec) = t;
79      y_plot(t_rec) = V;
80      y_plot_Iion(t_rec) = -Iion;
81      y_plot_INa(t_rec) = -INa;
82      y_plot_IK(t_rec) = -IK;
83      y_plot_IL(t_rec) = -IL;
84
85  end
86
87  toc
88
89  %% Plotting
90  figure()
91  set(gcf,'color','white')
92  set(gca,'fontsize',14)
93  cell = plot(x_plot,y_plot,'b');
94  legend('cell',2);
95  hold on;
96  y_plot_stim(1:Starttime/dt) = -80;
97  y_plot_stim(Starttime/dt+1:Endtime/dt+1) = -78;
98  y_plot_stim(Endtime/dt+2:EndOfSimulation/dt+1) = -80;
99  stimulus = plot(x_plot,y_plot_stim,'--k');
100 hold off;
101 legend([cell,stimulus],'cell','stimulus',2);
102 axis([0 EndOfSimulation -90 50]);
103 xlabel('Time (ms)');
104 ylabel('Voltage (mV)');
105
106 start = 157;
107 figure()
108 set(gcf,'color','white')
109 set(gca,'fontsize',14)
110 Na = plot(x_plot-start,y_plot_INa,'b');
111 hold on;
112 K = plot(x_plot-start,y_plot_IK,'r');
```

```
113 hold on;
114 L = plot(x_plot-start,y_plot_IL,'k');
115 hold on;
116 hold off;
117 legend([Na,K,L],'INa','IK','IL',2);
118 axis([0 10 -200 300]);
119 xlabel('Time (ms)');
120 ylabel('Current density (\muA/cm^2)');
```

**Listing B.2:** Host Code: LoadImageSeries.m

```
1  % Markus Micheal Hilscher - 0727932
2  % LoadImageSeries.m
3  % Loads the image series obtained by the AndorGUI program
4
5  % function Img = LoadImageSeries(filename)
6  %
7  % Reads the image series from a file, which was recorded by the program
8  % that records and stores the captured images by a camera
9  %
10 % Input:
11 % scalar "filename"
12 % contains the file name of the input file
13 %
14 % Output:
15 % matrix "Img"
16 % contains the grey values of a 32 x 32 matrix (image) times the values
17 % of frames
18
19 function Img = LoadImageSeries(filename)
20
21 eval (['load ',filename]); % executes the MATLAB string
22
23 Exposure % returns the exposure time in sec
24 Frames % returns the number of frames
25
26 x_width % returns the number of pixel of the x axis
27 y_height % returns the number of pixel of the y axis
28
29 Img = reshape(ret,x_width,y_height,Frames); % returns a M-by-N matrix whose
30                                             % elements are taken columnwise
```

**Listing B.3:** Host Code: mROI.m

```
function [m,x,y]=mROI(Img,first_pic,x,y)
%Calculate the mean change in fluorescence of a given region of interest
%Inputs: image series (Img), first_pic (the image in the data series
%that you wanna use for marking the ROI and x, y coordenates of the ROI.
%Enter 0 for both if you want to draw a new ROI.
[m,n,frames]=size(Img);
if length(x)<2
image(Img(:,:,first_pic),'CDataMapping','scaled')
colormap('jet')
loop=1;
cnt=1;
while loop==1
    [xx,yy,button]=ginput(1);
    if button==1
        x(cnt)=xx;
        y(cnt)=yy;
     if cnt>1
        a=line([x(cnt−1) x(cnt)],[y(cnt−1) y(cnt)]);
        set(a,'linewidth',2)
        set(a,'color','w')
     end
    cnt=cnt+1;
    end


    if button==3
        z=1
        a=line([x(1) x(cnt−1)],[y(1) y(cnt−1)]);
        set(a,'linewidth',2)
        set(a,'color','w')
        while z==1
        r=input('Redo (1=yes, 2=no)');
        if r==1 | r==2
            z=0;
        end
        end
        if r==2
            loop=0;
        end
        if r==1
            image(Img(:,:,first_pic),'CDataMapping','scaled')
            x=[];
            y=[];
```

```
44                  cnt=1;
45              end
46          end
47      end
48      end
49
50      Y=ones(m,n);
51      X=ones(m,n);
52      for ii=1:n
53          X(:,ii)=ii*X(:,ii);
54      end
55      for ii=1:m
56          Y(ii,:)=ii*Y(ii,:);
57      end
58      IN = inpolygon(X,Y,x,y);
59
60      image(IN.*double(Img(:,:,first_pic)),'CDataMapping','scaled');
61
62      gg=find(IN==1);
63      gg=length(gg);
64
65      for ii=1:frames
66          M=sum(sum(IN.*double(Img(:,:,ii))));
67          m(ii)=M/gg;
68      % mN(ii)=mean(Img(1:3,1:3,ii));
69      end
70
71      pause
72      %m=m-mN;
73      plot(m(2:length(m)))
74      m=m';
```

**Listing B.4:** Host Code: myrt_process.c

```
1   #include <linux/module.h> // header files for RTAI calculation
2   #include <asm/io.h> // and user space - kernel space communication
3   #include <math.h>
4   #include <rtai.h>
5   #include <rtai_sched.h>
6   #include <rtai_fifos.h>
7   #include <linux/comedi.h> // header files for data acquistion with the
8   #include <linux/comedilib.h> // complete interface of Comedi
9
10  #define TICK_PERIOD 50000 // tickrate: 50000 ns = 0.050 ms -> 20 kHz
```

```
11 #define TASK_PRIORITY 1 // priority to be given to the task, highest priority is 0
12 #define STACK_SIZE 10000 // size of the stack to e used by the new task
13 #define FIFO 0  // first in first out data structure
14 #define FIFO1 1  // for communication with user space
15 #define FIFO2 2
16 #define FIFO3 3
17 #define FIFO4 4
18 #define FIFO4 5
19 #define FIFO4 6
20 #define FACTOR 10/65536 // factor for the voltage output
21 #define TIMESTEP 0.05 // Euler step
22
23 static RT_TASK task; // real−time task
24 int subdevice = 0; // input subdevice
25 int chan = 0; // channel
26 int range = 1; // input range
27 int range1 = 2; // output range
28 int aref = AREF_DIFF; // reference of the device; differential inputs/outputs
29 comedi_t *device; // represent an open Comedi device
30 lsampl_t datab; // represent data values in libcomedi
31 int pdatab;  // data buffer for writing
32
33 // Model of a basket cell
34 float mv;  // membrane voltage in mV
35
36 float Iapp;  // stimulus in uA/cm^2
37 float INa;  // Na+ current
38 float IK;  // K+ current
39 float IL;  // leak current
40 float Iion;  // ionic current
41
42 float VNa = 55;  // reversal potential of the Na+ current in mV
43 float VK = −90;  // reversal potential of the K+ current in mV
44 float VL = −65;  // reversal potential of the leak current in mV
45
46 float gNa = 35;  // conductance of the Na+ current in mS/cm^2
47 float gK = 9;  // conductance of the K+ current in mS/cm^2
48 float gL = 0.1;  // conductance of the leak current in mS/cm^2
49
50 float k = 5;  // smaller k −> IK is slower −> AHP amplitude more negative
51 float Cmem = 1;  // membrane capacitance density in uF/cm^2
52
53 float h;  // inactivation varible h
```

```
54  float n;  // activation varible n
55  float minf;
56  float alpham;
57  float alphah;
58  float alphan;
59  float betam;
60  float betah;
61  float betan;
62
63  float time;  // time stamp
64
65  // Program
66  static void fun(int t)
67  {
68      while (1) {
69          rtf_get(FIFO1, &Iapp, sizeof(Iapp));
70          // get the stimulus value from the userspace
71          comedi_data_read(device,subdevice,chan,range,aref,&datab);
72          // read single sample from channel
73          // Comedi device, subdevice, channel, range, analog reference type, data
74          mv=100*((float)datab*FACTOR-5);
75          // converting voltages to samples
76
77          alpham = -0.1*(mv+35)/(exp(-0.1*(mv+35))-1);  // alpha m
78          alphah = 0.07*exp(-(mv+58)/20);  // alpha h
79          alphan = -0.01*(mv+34)/(exp(-0.1*(mv+34))-1);  // alpha n
80
81          betam = 4*exp(-(mv+60)/18);   // beta m
82          betah = 1/(exp(-0.1*(mv+28))+1);  // beta h
83          betan = 0.125*exp(-(mv+44)/80);   // beta n
84
85          minf = alpham/( alpham + betam );  // minf
86          h = h + TIMESTEP* k*(alphah*(1-h) - betah*h); // dh/dt
87          n = n + TIMESTEP* k*(alphan*(1-n) - betan*n); // dn/dt
88
89          INa = gNa*minf*minf*minf*h*(mv-VNa);  // Na+ current
90          IK = gK*n*n*n*n*(mv-VK);   // K+ current
91          IL = gL*(mv-VL);    // leakage current
92
93          Iion = INa + IK + IL;    // ionic current
94
95          pdatab=3.2768*iion+32768;     // converting samples to voltages
96          comedi_data_write(device,1,chan,range1,aref,pdatab);  // write single sample to channel
```

```
97          // device, subdevice, channel, range, analog reference type, data
98
99          rtf_put(FIFO, &mv, sizeof(mv));
100         // put the membrane voltage of the basket cell to the userspace
101         time = rt_get_cpu_time_ns();    // get the current time
102         rtf_put(FIFO2, &time, sizeof(time));   // put the time stamp to the userspace
103         rtf_put(FIFO3, &ina, sizeof(ina));
104         rtf_put(FIFO4, &ik, sizeof(ik));
105         rtf_put(FIFO5, &il, sizeof(il));
106         rtf_put(FIFO6, &iion, sizeof(iion));
107         rt_task_wait_period();    // wait until next period
108     }
109 }
110
111 int init_module(void)
112 {
113     RTIME tick_period;     // period timer
114     rt_set_periodic_mode();     // set timer mode
115     rt_task_init(&task, fun, 1, STACK_SIZE, TASK_PRIORITY, 1, 0); // create a periodic task
116     // task, task function, pass single integer value data, stack size, task priority, flag, signal
117     rtf_create(FIFO, 8000);     // create a real−time FIFO in kernel space
118     rtf_create(FIFO1, 8000);
119     rtf_create(FIFO2, 20000);
120     rtf_create(FIFO3, 8000);
121     rtf_create(FIFO4, 8000);
122     rtf_create(FIFO5, 8000);
123     rtf_create(FIFO6, 8000);
124
125     // start timer and periodic task
126     tick_period = start_rt_timer(nano2count(TICK_PERIOD));
127     // convert nanoseconds to internal count units and start timer
128     rt_task_make_periodic(&task, rt_get_time() + tick_period, tick_period);
129     // task gets suitable for periodic execution; task, start time (get the current time), period
130     mv = −64;      // membrane voltage at the beginning in mV
131     h = 0;      // inactivation varible h
132     n = 0;      // activation varible n
133     device=comedi_open("/dev/comedi0");    // open a Comedi device
134     comedi_data_read_hint(device,subdevice,chan,range,aref); // tell driver which channel is the next
135     // device, subdevice, channel, range, analog reference type
136     return 0;
137 }
138
139 void cleanup_module(void)
```

```
140 {
141     comedi_data_write(device,1,chan,0,aref,32768);
142     comedi_close(device);     // close a Comedi device
143     stop_rt_timer();      // stop timer
144     rtf_destroy(FIFO);      // close a real−time FIFO in kernel space
145     rtf_destroy(FIFO1);
146     rtf_destroy(FIFO2);
147     rtf_destroy(FIFO3);
148     rtf_destroy(FIFO4);
149     rtf_destroy(FIFO5);
150     rtf_destroy(FIFO6);
151     rt_task_delete(&task);     // delete a real−time task
152     return;
153 }
```

# Bibliography


Akemann, W., Mutoh, H., Perron, A., Rossier, J. and Knöpfel, T. 2010. Imaging brain electric signals with genetically targeted voltage-sensitive fluorescent proteins. *Nat. Methods.* 7:643-649.

Akemann, W., Mutoh, H., Perron, A., Kyung Park, Y., Iwamoto, Y. and Knöpfel, T. 2012. Imaging neural circuit dynamics with a voltage-sensitive fluorescent protein. *J. Neurophysiol.* 108:2323-2337.

Akerboom, J., Chen, T. W., Wardill, T. J., Tian, L., Marvin, J. S., Mutlu, S., Calderón, N. C., Esposti, F., Borghuis, B. G., Sun, X. R., Gordus, A., Orger, M. B., Portugues, R., Engert, F., Macklin, J. J., Filosa, A., Aggarwal, A., Kerr, R. A., Takagi, R., Kracun, S., Shigetomi, E., Khakh, B. S., Baier, H., Lagnado, L., Wang, S. S., Bargmann, C. I., Kimmel, B. E., Jayaraman, V., Svoboda, K., Kim, D.S., Schreiter, E. R. and Looger, L. L. 2012. Optimization of a GCaMP Calcium Indicator for Neural Activity Imaging. *J. Neurosci.* 32:13819-13840.

Arieli, A., Shoham, D., Hildesheim, R. and Grinvald, A. 1995. Coherent spatio-temporal pattern of on-going activity revealed by real time optical imaging coupled with single unit recording in the cat visual cortex. *J. Neurophysiol.* 73:2072-2093.

Baker, B. J., Mutoh, H., Dimitrov, D., Akemann, W., Perron, A., Iwamoto, Y., Jin, L., Cohen, L. B., Isacoff, E. Y., Pieribone, V. A., Hughes, T. and Knöpfel, T. 2008. Genetically encoded fluorescent sensors of membrane potential. *Brain Cell Biol.* 36:53-67.

Bedlack, R. S. Jr., Wei, M. and Loew L. M. 1992. Localized membrane depolarizations and localized calcium influx during electric field-guided neurite growth. *Neuron.* 9:393-403.

Berger, T., Borgdorff, A., Crochet, S., Neubauer, F.B., Lefort, S., Fauvet, B., Ferezou, I., Carleton, A., Lüscher, H. R. and Petersen C. C. 2007. Combined voltage and calcium epifluorescence imaging in vitro and in vivo reveals subthreshold and suprathreshold dynamics of mouse barrel cortex. *J. Neurophysiol.* 97:3751-3762.

Bianchi, R. and Wong, R. K. 1994. Carbachol-induced synchronized rhythmic bursts in CA3 neurons of guinea pig hippocampus in vitro. *J. Neurophysiol.* 72:131-138.

Bradley, J., Luo, R., Otis, T. S. and DiGregorio, D. A. 2009. Submillisecond Optical Reporting of Membrane Potential In Situ Using a Neuronal Tracer Dye. *J. Neurosci.* 29:9197-9209.

Brown, C. J., Abbas, P.J., Borland, J. and Bertschy M. R. 1996. Electrically evoked whole nerve action potentials in Ineraid cochlear implant users: responses to different stimulating electrode configurations and comparison to psychophysical responses. *J. Speech Hear. Res.* 39:453-467.

Burns, S. P., Xing, D. and Shapley, R. M. 2010. Comparisons of the dynamics of local field potential and multiunit activity signals in macaque visual cortex. *J. Neurosci.* 30:13739-13749.

Buzsáki , G., Anastassiou, C. A. and Koch, C. 2012. The origin of extracellular fields and currents - EEG, ECoG, LFP and spikes. *Nature Rev. Neurosci.* 13:407-420.

Canepari, M., Vogt, K. and Zecevic, D. 2008. Combining voltage and calcium imaging from neuronal dendrites. *Cell Mol. Neurobiol.* 28:1079-1093.

Canepari, M. and Zecevic, D. 2010. Membrane Potential Imaging in the Nervous System. *Springer.*

Chudakov, D. M., Matz, M. V., Lukyanov, S. and Lukyanov, K. A. 2010. Fluorescent Proteins and Their Applications in Imaging Living Cells and Tissues. *Physiol Rev.* 90:1103-1163.

Daya, R.N and Davidson, M.W. 2009. The fluorescent protein palette: tools for cellular imaging. *Chem. Soc. Rev.* 38:2887-2921.

Dimitrov, D., He, Y., Mutoh, H., Baker, B. J., Cohen, L., Akemann, W. and Knöpfel, T. 2007. Engineering and Characterization of an Enhanced Fluorescent Protein Voltage Sensor. *PLoS ONE.* 2:e440.

Dixit, R. and Cyr, R. 2003. Cell damage and reactive oxygen species production induced by fluorescence microscopy: effect on mitosis and guidelines for non-invasive fluorescence microscopy. *The Plant. Journal.* 36:280-290.

Doering, L. C. 2010. Protocols for Neural Cell Culture. Fourth Edition. *Springer Protocols Handbooks.*

Dugué, G. P., Akemann, W. and Knöpfel, T. 2012. A comprehensive concept of optogenetics. *Prog. Brain Res.* 196:1-28.

Ferezou, I., Bolea, S. and Petersen, C.C. 2006. Visualizing the cortical representation of whisker touch: voltage-sensitive dye imaging in freely moving mice. *Neuron.* 50:617-629.

Fetcho, J. R., Cox, K. J. and O'Malley, D. M. 1998. Monitoring activity in neuronal populations with single-cell resolution in a behaving vertebrate. *Histochem. J.* 30:153-167.

Förster T. 1948. Intermolecular Energy Migration and Fluorescence. *Ann. Phys.* 2:55-75.

Fluhler, E., Burnham, V. G. and Loew, L. M. 1985. Spectra, membrane binding, and potentiometric responses of new charge shift probes. *Biochemistry.* 24:5749-5755.

Fukuda, S., Kato, F., Tozuka, Y., Yamaguchi, M., Miyamoto, Y. and Hisatsune, T. 2003. Two distinct subpopulations of nestin-positive cells in adult mouse dentate gyrus. *J. Neurosci.* 23:9357-9366.

Gautam, S. G., Perron, A., Mutoh, H. and Knöpfel, T. 2009. Exploration of fluorescent protein voltage probes based on circularly permuted fluorescent proteins. *Front Neuroeng.* 2:14.

Gersdorff, H. and Borst, J. G. 2001. Short-term plasticity at the calyx of held. *Nat. Rev. Neurosci.* 3:53-64.

Grinvald, A., Manker, A. and Segal, M. 1982. Visualization of the spread of electrical activity in rat hippocampal slices by voltage-sensitive optical probes. *J. Physiol.* 333:269-291.

Grinvald, A. and Hildesheim, R. 2004. VSDI: a new era in functional imaging of cortical dynamics. *Nat. Rev. Neurosci.* 5:874-885.

Gross, E., Bedlack, R. S. Jr. and Loew, L. M. 1994. Dual-wavelength ratiometric fluorescence measurement of the membrane dipole potential. *Biophys. J.* 67:208-216.

Hagenston, A. M. and Bading, H. 2011. Calcium signaling in synapse-to-nucleus communication. *Cold Spring Harb. Perspect. Biol.* 3:a004564.

Halliday, D., Resnick, R. and Walker, J. 2011. Fundamentals of Physics, Nineth Edition. *John Wiley & Sons.*

Halliday, D., Resnick, R. and Walker, J. 2010. Applications of Spectrophotometry. Quantitative Chemical Analysis (8th ed.) *New York: W. H. Freeman and Co.*

Hell, S. W., Stelzer, E. H. K., Lindek, S. and Cremer, C. 1994. Confocal microscopy with an increased detection aperture: type-B 4Pi confocal microscopy. *Opt. Lett.* 19:222-224.

Held P. 2006. An Introduction to Fluorescence Resonance Energy Transfer (FRET) Technology and its Application in Bioscience. *BioTek Application Note.*

Higley M. J. and Sabatini, B. L. 2008. Calcium signaling in dendrites and spines: practical and functional considerations. *Neuron.* 59:902-913

Hille, B. 1992. Pumping ions. *Science.* 255:742

Hilscher M. M. 2012. Real Time Processing and Synchronization in Hybrid Hippocampal Microcircuits. *Master's Thesis. Vienna University of Technology. Institute for Analysis and Scientific Computing.*

Hires, S. A., Tian, L. and Looger, L. L. 2008. Reporting neural activity with genetically encoded calcium indicators. *Brain Cell Biol.* 36:69-86.

Hodgkin, A. L. and Huxley, A. F. 1952. A quantitative description of membrane current and its application to conduction and excitation in nerve. *J. Physiol.* 117:500-544.

Horikawa, K., Yamada, Y., Matsuda, T., Kobayashi, K., Hashimoto, M., Matsura, T., Miyawaki, A., Michikawa, T., Mikoshiba K. and Nagai T. 2010. Spontaneous network activity visualized by ultrasensitive Ca(2+) indicators, yellow Cameleon-Nano. *Nat. Methods.* 7:729-732.

Jaffe, D. B., Johnston, D., Lasser, R. N., Lisman, J. E., Miyakawa, H. and Ross, W. N. 1992. The spread of Na+ spikes determines the pattern of dendritic Ca2+ entry into hippocampal neurons. *Nature.* 357:244-246.

Ji, N., Shroff, H., Zhong, H. and Betzig, E. 2008. Advances in the speed and resolution of light microscopy. *Curr. Opin. Neurobiol.* 18:605-616.

Kajikawa, Y. and Schroeder, C. E. 2011. How local is the local field potential? *Neuron.* 72:847-858.

Knöpfel, T., Díez-García, J. and Akemann, W. 2006. Optical probing of neuronal circuit dynamics: genetically encoded versus classical fluorescent sensors. *Trends Neurosci.* 29:160-166.

Knöpfel, T., Lin, M. Z., Levskaya, A., Tian, L., Lin, J. Y. and Boyden E. S. 2010. Toward the second generation of optogenetic tools. *J. Neurosci.* 30:14998-15004.

Knöpfel, T. 2012. Genetically encoded optical indicators for the analysis of neuronal circuits. *Nat. Rev. Neurosci.* 13:687-700.

Kremers G. J., Gilbert S. G., Cranfill P. J., Davidson M.W. and Piston D. W. 2011. Fluorescent proteins at a glance. *J. Cell Sci.*124:157-160.

Leão, R. N., Tan, H. M. and Fisahn, A. 2009. Kv7/KCNQ Channels Control Action Potential Phasing of Pyramidal Neurons During Hippocampal Gamma Oscillations In Vitro. *J. Neurosci.* 29:13353-13364.

Loew, L. M., Cohen, L. B., Dix, J., Fluhler, E. N., Montana, V., Salama, G. and Wu, J. Y. 1992. A naphthyl analog of the aminostyryl pyridinium class of potentiometric membrane dyes shows consistent sensitivity in a variety of tissue, cell, and model membrane preparations. *J. Membr. Biol.* 130:1-10.

Lytton, W. W. and Kerr, C.C. 2006. Computational neuroscience of the neuron.

Mank, M. and Griesbeck, O. 2008. Genetically encoded calcium indicators. *Chem Rev.* 108:1550-1564.

Mao, T., O'Connor, D. H., Scheuss, V., Nakai, J. and Svoboda, K. 2008. Characterization and subcellular targeting of GCaMP-type genetically-encoded calcium indicators. *PLoS One.* 3:e1796.

Maravall, M., Mainen, Z. F., Sabatini, B.L. and Svoboda, K. 2000. Estimating intracellular calcium concentrations and buffering without wavelength ratioing. *Biophys. J.* 78:2655-2667.

Martin, G. 2007. Keck Microscopy Facility. *University of Washington.*

McCombs, J. E. and Palmer, A. E. 2008. Measuring calcium dynamics in living cells with genetically encodable calcium indicators. *Methods.* 46:152-159.

Miyawaki, A. and Tsien, R.Y. 2000. Monitoring protein conformations and interactions by fluorescence resonance energy transfer between mutants of green fluorescent protein. *Methods Enzymol.* 327: 472-500.

Molleman, A., 2003. Patch Clamping: An Introductory Guide To Patch Clamp Electrophysiology. *John Wiley & Sons, Ltd.*

Munguba H. 2013. Genetically encoded calcium and voltage indicators in the detection of action potentials and synaptic inputs in cultured hippocampal neurons. *Master's Thesis. Federal University of Rio Grande do Norte. Brain Institute.*

Mutoh, H., Perron, A., Dimitrov, D., Iwamoto, Y., Akemann, W., Chudakov, D. M. and Knöpfel, T. 2009. Spectrally-resolved response properties of the three most advanced FRET based fluorescent protein voltage probes. *PLoS ONE.* 4:e4555.

Mutoh, H., Perron, A., Akemann, W., Iwamoto and Knöpfel, T. 2011. Optogenetic monitoring of membrane potentials. *Exp Physiol.* 96:13-8.

Müller, W. and Connor, J. A. 1991. Dendritic spines as individual neuronal compartments for synaptic Ca2+ responses. *Nature.* 354:73-76.

Neher, E. and Sakmann, B. 1976. Single-channel currents recorded from membrane of denervated frog muscle fibres. *Nature.* 260:799-802.

Nunez, J 2008. Primary Culture of Hippocampal Neurons from P0 Newborn Rats. *J. Vis. Exp.* 19:e895.

Obaid, A. L., Loew, L. M., Wuskell, J. P. and Salzberg, B. M. 2004. Novel naphthylstyryl-pyridium potentiometric dyes offer advantages for neural network analysis. *J. Neurosci. Methods.* 134:179-190.

Perron, A., Mutoh, H., Akemann, W., Gautam, S. G., Dimitrov, D., Iwamoto, Y. and Knöpfel, T. 2009. Second and third generation voltage-sensitive fluorescent proteins for monitoring membrane potential. *Front. Mol. Neurosci.* 2:5.

Perron, A., Akemann, W., Mutoh, H. and Knöpfel, T. 2012. Genetically encoded probes for optical imaging of brain electrical activity. *Prog. Brain Res.* 196:63-77.

Purves, D., Augustine, G. J., Fitzpatrick, D., Hall, W. C., LaMantia, A.-S., McNamara, J. O., and White L. E. 2004. Neuroscience, Fourth Edition. *Sinauer Associates.*

Rattay, F. 1999. The basic mechanism for the electrical stimulation of the nervous system. *Neuroscience.* 89:335-346

Rattay, F. and Wenger, C. 2010. Which elements of the mammalian central nervous system are excited by low current stimulation with microelectrodes? *Neuroscience.* 170:399-407.

Rattay, F., Paredes, L. P. and Leão, R. N. 2012. Strength-duration relationship for intra- versus extracellular stimulation with microelectrodes. *Neuroscience.* 214:1-13.

Sakai, R., Repunte-Canonigo, V., Raj, C. D. and Knöpfel T. 2001. Design and characterization of a DNA-encoded, voltage-sensitive fluorescent protein. *Eur. J. Neurosci.* 13:2314-2318.

Scanziani and Häusser. 2009. Electrophysiology in the age of light. *Nature.* 461:930-939.

Shcherbo, D., Merzlyak, E. M., Chepurnykh, T. V., Fradkov, A. F., Ermakova, G. V., Solovieva, E. A., Lukyanov, K. A., Bogdanova, E. A., Zaraisky, A. G., Lukyanov, S. and Chudakov, D. M. 2007. Bright far-red fluorescent protein for whole-body imaging. *Nat. Methods.* 4:741-746.

Shcherbo, D., Murphy, C. S., Ermakova, G. V., Solovieva, E. A., Chepurnykh, T. V., Shcheglov, A. S., Verkhusha, V. V., Pletnev, V. Z., Hazelwood, K. L., Roche, P. M., Lukyanov, S., Zaraisky, A. G., Davidson, M. W. and Chudakov, D. M. 2009. Far-red fluorescent tags for protein imaging in living tissues. *Biochem. J.* 418:567-574.

Shimormura, O., Johnson, F. H. and SAIGA, Y. 1962. Extraction, purification and properties of aequorin, a bioluminescent protein from the luminous hydromedusan, Aequorea. *J. Cell Comp. Physiol.* 59:223-39.

Svoboda, K., Denk, W., Kleinfeld, D. and Tank, D. W. 1997. In vivo dendritic calcium dynamics in neocortical pyramidal neurons. *Nature.* 385:161-165.

Taniguchi, Y., Ikehara, T., Kamo, N., Watanabe, Y., Yamasaki, H. and Toyoshima, Y. 2007. Application of fluorescence resonance energy transfer (FRET) to investigation of light-induced conformational changes of the phoborhodopsin/transducer complex. *Photochem. Photobiol.* 83:311-316.

Tian, L. and Looger, L. L. 2008. Genetically encoded fluorescent sensors for studying healthy and diseased nervous systems. *Drug Discov. Today Dis. Models.* 5:27-35.

Tian, L., Hires, S. A., Mao, T., Huber, D., Chiappe, M. E., Chalasani, S. H., Petreanu, L., Akerboom, J., McKinney, S. A., Schreiter, E. R., Bargmann, C. I., Jayaraman, V., Svoboda, K. and Looger, L. L. 2009. Imaging neural activity in worms, flies and mice with improved GCaMP calcium indicators. *Nature Methods.* 6:875-881.

Tsien, R. Y. 1998. The green fluorescent protein. *Ann. Review Biochem.* 67:509-544.

Tro, N. 2009. Chemistry in Focus : A Molecular View of Our World, Fourth Edition. *Cengage Learning - Brooks/Cole.*

Verkhratsky, A., Krishtal, O. A. and Petersen, O. H. 2006. From Galvani to patch clamp: the development of electrophysiology. *European Journal of Physiology.* 453:233-247.

Villalba-Galea, C. A., Miceli, F., Taglialatela, M. and Bezanilla, F. 2009. Coupling between the voltage-sensing and phosphatase domains of Ci-VSP. *J. Gen. Physiol.* 134: 5-14.

Vogelstein, J.T., Watson, B.O., Packer, A.M., Yuste, R., Jedynak, B. and Paninski, L. 2009. Spike inference from calcium imaging using sequential Monte Carlo methods. *Biophys. J.* 97:636-55.

Wang, X.-J. and Buzsáki, G. 1996. Gamma Oscillation by Synaptic Inhibition in a Hippocampal Interneuronal Network Model. *J. Neurosci.* 16:6402-6413.

Wilson, H. A., Seligmann, B. E. and Chused, T. M. 1985. Voltage-sensitive cyanine dye fluorescence signals in lymphocytes: plasma membrane and mitochondrial components. *J. Cell Physiol.* 125:61-71.

Yaksi, E. and Friedrich, R.W. 2006. Reconstruction of firing rate changes across neuronal populations by temporally deconvolved Ca2+ imaging. *Nat. Methods.* 3:377-383.

Yamada, Y., Michikawa, T., Hashimoto, M., Horikawa, K., Nagai, T., Miyawaki, A., Häusser, M. and Mikoshiba, K. 2011. Quantitative comparison of genetically encoded Ca2+ indicators in cortical pyramidal cells and cerebellar purkinje cells. *Front. Cell. Neurosci.* 5:18.

Yamada, Y. and Mikoshiba, K. 2012. Quantitative comparison of novel GCaMP-type genetically encoded Ca2+ indicators in mammalian neurons. *Front. Cell. Neurosci.* 6:41.

Zhang, F., Prigge, M., Beyriere, F., Tsunoda, S. P., Mattis, J., Yizhar, O., Hegemann, P. and Deisseroth, K. 2008. Red-shifted optogenetic excitation: a tool for fast neural control derived from Volvox carteri. *Nat. Neurosci.* 11:631-633.

Zhao, Y., Araki, S., Wu, J., Teramoto, T., Chang, Y. F., Nakano, M., Abdelfattah, A. S., Fujiwara, M., Ishihara, T., Nagai, T. and Campbell, R. E. 2011. An expanded palette of genetically encoded $Ca^{2+}$ indicators. *Science.* 333:1888-1891.